# A Central Pattern Generator Producing Alternative Outputs: Temporal Pattern of Premotor Activity

**Brian J. Norris, Adam L. Weaver, Lee G. Morris, Angela Wenning, Paul A. García and Ronald L. Calabrese**

*J Neurophysiol* 96:309-326, 2006. First published Apr 12, 2006; doi:10.1152/jn.00011.2006



***Journal of Neurophysiology*** publishes original articles on the function of the nervous system. It is published 12 times a year (monthly) by the American Physiological Society, 9650 Rockville Pike, Bethesda MD 20814-3991.  ISSN: 0022-3077, ESSN: 1522-1598. Visit our website at http://www.the-aps.org/.

*J Neurophysiol* 96: 309–326, 2006.
First published April 12, 2006; doi:10.1152/jn.00011.2006.

# A Central Pattern Generator Producing Alternative Outputs: Temporal Pattern of Premotor Activity

**Brian J. Norris,[1,2,*] Adam L. Weaver,[1,*] Lee G. Morris,[1] Angela Wenning,[1] Paul A. García,[1] and Ronald L. Calabrese[1]**

[1]*Department of Biology, Emory University, Atlanta, Georgia; and* [2]*Department of Biological Sciences, California State University, San Marcos, California*

Submitted 5 January 2006; accepted in final form 3 April 2006

**Norris, Brian J., Adam L. Weaver, Lee G. Morris, Angela Wenning, Paul A. García, and Ronald L. Calabrese.** A central pattern generator producing alternative outputs: temporal pattern of premotor activity. *J Neurophysiol* 96: 309–326, 2006. First published April 12, 2006; doi:10.1152/jn.00011.2006. The central pattern generator for heartbeat in medicinal leeches constitutes seven identified pairs of segmental heart interneurons. Four identified pairs of heart interneurons make a staggered pattern of inhibitory synaptic connections with segmental heart motor neurons. Using extracellular recording from multiple interneurons in the network in 56 isolated nerve cords, we show that this pattern generator produces a side-to-side asymmetric pattern of intersegmental coordination among ipsilateral premotor interneurons. This pattern corresponds to a similarly asymmetric fictive motor pattern in heart motor neurons and asymmetric constriction pattern of the two tubular hearts, synchronous and peristaltic. We provide a quantitative description of the firing pattern of all the premotor interneurons, including phase, duty cycle, and intraburst frequency of this premotor activity pattern. This analysis identifies two stereotypical coordination modes corresponding to synchronous and peristaltic, which show phase constancy over a broad range of periods as do the fictive motor pattern and the heart constriction pattern. Coordination mode is controlled through one segmental pair of heart interneurons (switch interneurons). Side-to-side switches in coordination mode are a regular feature of this pattern generator and occur with changes in activity state of these switch interneurons. Associated with synchronous coordination of premotor interneurons, the ipsilateral switch interneuron is in an active state, during which it produces rhythmic bursts, whereas associated with peristaltic coordination, the ipsilateral switch interneuron is largely silent. We argue that timing and pattern elaboration are separate functions produced by overlapping subnetworks in the heartbeat central pattern generator.

## INTRODUCTION

Repetitive and rhythmic motor patterns, both episodic and continuous, are thought to derive significantly from repetitively or rhythmically active central neuronal networks called *central pattern generators* (CPGs; Marder and Bucher 2001; Marder and Calabrese 1996). Particularly in invertebrates, where analysis has been greatly facilitated by the ability to identify many of the key neuronal elements (mostly interneurons) composing a pattern generator, it has been possible to record and to biophysically analyze these elements and their synaptic interactions (Marder et al. 2005). As previously indicated by Marder and colleagues (2005), however, this level of cellular understanding of itself "is only a starting point to understanding the dynamics of circuit operation." Modeling has been essential to thorough analysis of CPG networks (for recent reviews see De Schutter et al. 2005; Marder et al. 2005). Although much progress is now being made identifying the key neuronal elements that make up pattern generators in vertebrates, the real circuitry involved in any particular pattern generator is far from certain. In only a few vertebrate systems is enough known so that mathematical/computer models can be constructed that generate specific hypotheses about network function (Butera et al. 1999a,b; Del Negro et al. 2001; Hellgren-Kotaleski et al. 1999a,b; Rybak et al. 2004a,b; Tunstall et al. 2002).

One of our long-range aims is a complete model of how a CPG controls motor outflow. After element identification, circuit description, and biophysical analysis, the entrée to such a model must be a quantitative assessment of the activity relations of the premotor elements that drive motor neuron activity to produce the fictive motor pattern. Such a description, however, has not been forthcoming except for the crustacean stomatogastric motor patterns that control the decapod pylorus and gastric mill (Bucher et al. 2005; Hooper 1997a,b; Marder and Bucher 2001; Marder and Calabrese 1996; Marder et al. 2005). Here, many of the main pattern-generating elements are motor neurons themselves and the network is numerically restricted. These networks, particularly the one controlling the gastric mill, are remarkably plastic in their output producing myriad subpatterns according to modulatory state so that normative activity analogous, say, to steady swimming in still water or heartbeat at rest, may not exist, and emphasis has been on mechanistically explaining variation (Hooper and DiCaprio 2004; Marder and Bucher 2001; Marder et al. 2005; Nusbaum and Beenhakker 2002). Other motor pattern generators have been analyzed for activity pattern but not quantitatively (e.g., Katz et al. 2004; Kristan et al. 2005; Mulloney et al. 1998; Straub et al. 2002). Moreover, for fruitful generalization and comparison across networks, the activity pattern of each particular pattern generator must be independently described and its network dynamic analyzed.

It has long been speculated (e.g., Grillner 1981, 2003; Grillner et al. 2005; Marder and Bucher 2001; Stein 2005) that the rhythm-generating and pattern-forming functions of a CPG may be separated at least conceptually, if not by assigning different neuronal elements to each aspect. Here *rhythm* refers to the basic timing oscillation in a pattern generator, whereas

* B. J. Norris and A. L. Weaver contributed equally to this work.
Address for reprint requests and other correspondence: R. L. Calabrese, Dept. of Biology, Emory University, 1510 Clifton Road N.E., Atlanta, GA 30322 (E-mail: rcalabre@biology.emory.edu).

The costs of publication of this article were defrayed in part by the payment of page charges. The article must therefore be hereby marked "*advertisement*" in accordance with 18 U.S.C. Section 1734 solely to indicate this fact.

*pattern* refers to the elaboration of this timing rhythm into a functional motor program organized both spatially and temporally. Our current level of understanding suggests that many neuronal elements serve in both functions (Hooper and DiCaprio 2004; Kristan et al. 2005; Marder et al. 2005). For example, some pattern generators produce segmentally distributed output, such as that controlling undulatory swimming (Cang and Friesen 2000, 2002; De Schutter et al. 2005; Grillner et al. 2005; Kristan et al. 2005), so that a conceptual separation between rhythm generation as expressed in side-to side or dorsal–ventral alternation and pattern formation as expressed in intersegmental coordination seems clear, although key elements involved in intersegmental coordination appear integral to rhythm generation. The crayfish swimmeret system stands in stark contrast here with network elements clearly separated along these functional lines (Mulloney et al. 1998, 2006; Paul and Mulloney 1985). Clearly separating these functions in any given circuit may help us extract useful generalization for other networks controlling similar movements and again quantitative assessment of network activity is a necessary step.

Motor pattern-generating networks can produce motor variants that reflect changes in coordination between motor elements necessary for opposing functions, as for example egestive versus ingestive biting behavior in the mollusk *Aplysia* (Cropper et al. 2004; Hurwitz and Susswein 1996). A quantitative assessment of network activity during the alternative forms of circuit output is necessary for assessing how such alternative circuit outputs are brought about.

The heartbeat CPG of the medicinal leech has been studied intensively for over two decades, yet a quantitative description of its activity pattern has not been forthcoming (for a recent review see Kristan et al. 2005). In large part, this was attributable to the application of intracellular recording techniques that limit the number of interneuronal elements that can be easily recorded simultaneously and alter the activity of the elements by introducing penetration-associated leak (Cymbalyuk et al. 2002). Now that extracellular recording from multiple interneurons in the network is routine no obstacle exists for a more quantitative description (Masino and Calabrese 2002a,b,c).

The leech has two tubular hearts running the length of the body and moving blood through its closed circulatory system (Krahl and Zerbst-Boroffka 1983; Thompson and Stent 1976a; Wenning et al. 2004a). The beating pattern (beat period 4–10 s) is asymmetric with one heart generating high systolic pressure through a front-directed peristaltic wave (peristaltic coordination mode) along its length, and the other generating low systolic pressure through near synchronous constriction (synchronous coordination mode) along its length. The peristaltic heart moves blood forward, whereas the synchronous heart has been hypothesized mainly to push blood into the peripheral circulation (Hildebrandt 1988; Wenning et al. 2004a). After about 20 to 40 beats (switch period about 100–400 s) the hearts switch roles (Krahl and Zerbst-Boroffka 1983; Thompson and Stent 1976a; Wenning et al. 2004a). This constriction pattern and the regular switches in coordination mode were previously quantitatively described in detail (Wenning et al. 2004a).

Heart motor neurons occur as bilateral pairs in the midbody segmental ganglia 3 through 18 (G3–G18). Each motor neuron innervates the segmental section of its ipsilateral heart tube and drives and entrains the beating of the heart in its segment (Maranto and Calabrese 1984a,b). In the isolated nervous system, the bursting discharge pattern of this ensemble of segmental motor neurons (HE motor neurons) reflects well the segmental constriction pattern of the hearts and the switches in coordination mode (Wenning et al. 2004b). This asymmetric pattern of motor outflow has been quantified as to intersegmental phase relations, duty cycle, and intraburst spike frequency (Wenning et al. 2004b).

The central pattern generator for heartbeat consists of seven identified pairs of segmental heart interneurons located in the first seven midbody segmental ganglia (G1–G7) (Fig. 1); one as yet unidentified pair of heart interneurons is known to exist—its cell body has not been identified, so it cannot be associated with a segmental ganglion, and thus is referred to with the ganglionic index X (Calabrese 1977; Thompson and Stent 1976b,c ). Of the identified interneurons the pairs in G3 and G4, and G6 and G7 are premotor (front and rear premotor

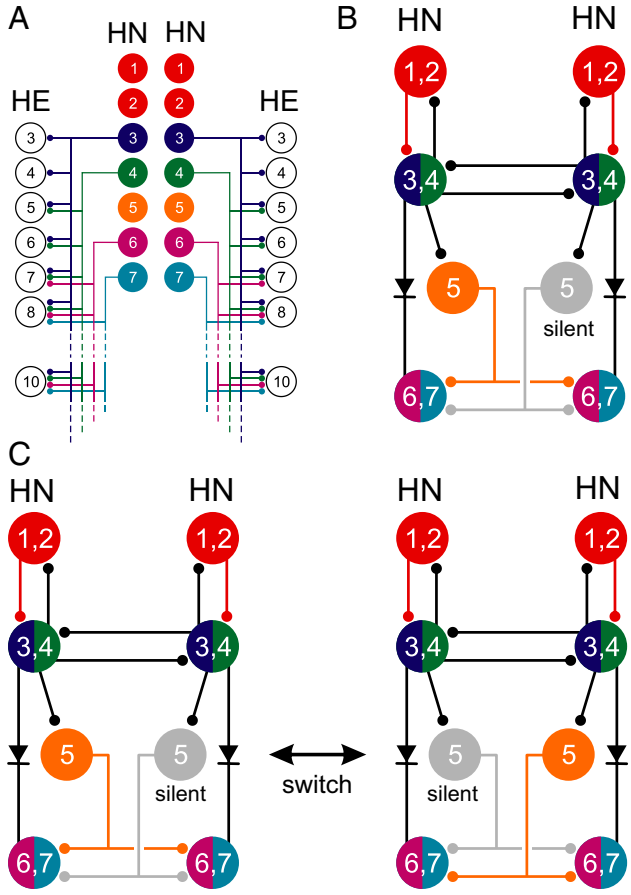


FIG. 1. Network diagrams for the leech heart beat central pattern generator (CPG) and associated heart motor neurons. *A*: all the identified interneurons (HN) of the CPG and their pattern of synaptic connections to motor neurons (HE). G3, G4, G6, and G7 interneurons are premotor interneurons. *B*: circuit diagram showing synaptic connections among interneurons of the heartbeat CPG. *C*: switches in coordination mode of the heartbeat CPG are associated with switches in which the G5 interneuron (switch interneuron) is active (color) and which is silent (gray). In all panels, large colored circles are cell bodies and associated input processes. Lines indicate cell processes, small colored/black circles indicate inhibitory chemical synapses, and diodes indicate rectifying electrical synapses. For simplicity in the CPG diagrams of *B* and *C* cells with similar input and output, connections and function are lumped. Colors chosen are used to designate associated electrophysiological traces and analysis throughout (see METHODS for color code).

interneurons, respectively), making inhibitory synapses in a staggered pattern with ipsilateral motor neurons by a posterior directed axon (Fig. 1*A*) (Thompson and Stent 1976b). The heart interneurons interact with one another by inhibitory synapses and electrical junctions that appear to be rectifying (Calabrese 1977, 1979; Thompson and Stent 1976c) (Fig. 1*B*). The first four pairs of heart interneurons can all reset and entrain the activity of the entire pattern generator when driven with injected current pulses, whereas the rear interneurons cannot (Masino and Calabrese 2002c; Peterson and Calabrese 1982). Thus this core of interneurons (in G1–G4) constitutes a beat-timing network for the pattern generator. This timing network has been examined in detail and its phase relations, duty cycle, and intraburst spike frequency described quantitatively (Masino and Calabrese 2002a,b,c). Within the timing network, strong reciprocal inhibitory synapses between the interneuron pairs in G3 and G4 and intrinsic membrane properties produce rhythmic bursting activity (the front premotor interneurons, in G3 and G4, are consequently also referred to as oscillator interneurons) and sets up strict side-to-side alternation and symmetry in the timing network activity pattern. The phase relations between the G3 and G4 pairs are somewhat plastic; each can be considered an independent half-center oscillator coordinated by the G1 and G2 heart interneurons (coordinating interneurons) so that the faster half-center oscillator leads in phase (Masino and Calabrese 2002a,b), yet there is strict right–left symmetry and in the majority of preparations the G4 half-center oscillator leads in phase. The timing network is linked to the rear premotor interneurons through direct ipsilateral electrical connections and indirectly through bilateral inhibitory connections from the heart interneuron pair in G5 (Fig. 1*B*). The G5 interneurons are called *switch interneurons* because bilateral recordings (Calabrese and Peterson 1983; Lu et al. 1999) show one active in rhythmic bursts and one largely silent with reciprocal switches in activity state (Fig. 1*C*). These switches in the activity state have been extensively observed unilaterally and were studied using voltage clamp (Gramoll et al. 1994). The silent state is associated with a leaklike conductance with reversal potential near −60 mV that suppresses spike activity (Gramoll et al. 1994). The active state of the switch interneuron is associated with the synchronous coordination state and the silent state with the peristaltic coordination state (Calabrese 1977; Calabrese and Peterson 1983). The switch interneurons do not appear to be able to switch autonomously, and it is hypothesized that the neuron that is silent is under the control of a switch oscillator extrinsic to the known heart interneurons (Lu et al. 1999).

Given that the timing network produces side-to-side symmetric output, it is clear that the necessary asymmetries in output of the premotor interneurons to the motor neurons to generate their two different coordination states and the switching between them arise from the asymmetric and variable phasing of the rear premotor interneurons. The activity of these interneurons with respect to the timing network and the switch interneurons is known only in the most general way, resulting from a limited number of pairwise intracellular recordings (Calabrese 1977; Thompson and Stent 1976c). Thus the major focus of this study was to provide a quantitative description of the firing pattern of all the premotor interneurons and the switch interneurons—including phase, duty cycle, and intraburst frequency—and to compare this activity pattern to the fictive motor program for heartbeat (Wenning et al. 2004b). This analysis identifies two stereotypical coordination modes corresponding to synchronous and peristaltic coordination in the fictive motor program and shows that these coordination modes exhibit phase constancy over a broad range of periods. We also explore switching and show that associated with synchronous coordination of premotor interneurons, the ipsilateral switch interneuron is in an active state, during which it produces rhythmic bursts, whereas associated with peristaltic coordination, the ipsilateral switch interneuron is largely silent. Side-to-side switches in coordination mode are a regular feature of this pattern generator and are associated with changes in activity state of the switch interneurons. We argue that timing and pattern elaboration are indeed separate functions produced by overlapping subnetworks in the leech heartbeat central pattern generator.

## METHODS

### *Animals and solutions*

Leeches (*Hirudo medicinalis*) were obtained from commercial suppliers (Leeches USA, Westbury, NY and Biopharm, Charleston, NC) and maintained in artificial pond water at 15°C. After the animals were anesthetized in cold saline, chains of ganglia were dissected consisting of the head brain (HB) to at least midbody ganglion 15 (G15) for recording the heart interneuron activity rhythm and G2 to G8 for recording the X heart interneuron IPSC pattern in heart motor neurons. Extra ganglia were in some cases left attached to these later preparations for pinning purposes but the connectives to these ganglia were thoroughly crushed. The preparations were pinned (ventral surface up) in 60-mm petri dishes lined with Sylgard (Dow Corning, Midland, MI). Ganglia in which heart interneurons or heart motor neurons were to be recorded were desheathed using fine scissors or microscalpels. Heart interneurons were identified based on soma size, soma location in the ganglion, and ultimately identified by their characteristic bursting activity (Fig. 2*A*). The preparation was continuously superfused with normal leech saline containing (in mM): 115 NaCl, 4 KCl, 1.8 $CaCl_2$, 10 glucose, 10 HEPES buffer, adjusted to pH 7.4 with NaOH, at 1–2 ml/min (bath volume 6–8 ml). Previous experience has indicated that the heart interneuron X activity pattern associated with synchronous coordination is sensitive to prolonged dissection and extensive desheathing of ganglia; thus when recording the X heart interneuron's IPSCs, all attempts were made to keep dissections <1 h and to minimize the number of ganglia desheathed. Moreover, those preparations where the X heart interneuron IPSP pattern never switched out of the peristaltic state during the course of an experiment (often despite documented switches in the identified rear premotor interneurons) were discarded.

### *Extracellular and intracellular recording techniques*

For intracellular voltage-clamp recordings from heart motor neurons, we used sharp intracellular electrodes (about 20–30 MΩ filled with 4 M KAc, 20 mM KCl) following the methods described in Opdyke and Calabrese (1995). Briefly, voltage-clamp experiments were performed using an Axoclamp-2A amplifier (Axon Instruments, Union City, CA) operating in discontinuous current-clamp or discontinuous single-electrode voltage-clamp mode with a sample rate of 2.5–2.8 kHz. The electrode potential was monitored to ensure that it settled during each sample cycle. Output bandwidth was 0.3 kHz. Voltage-clamp gain was 0.8 to 2.0 nA/mV. Holding potential for recording spontaneous IPSCs in motor neurons was −45 mV in all experiments (except those in which X-mediated IPSCs were recorded

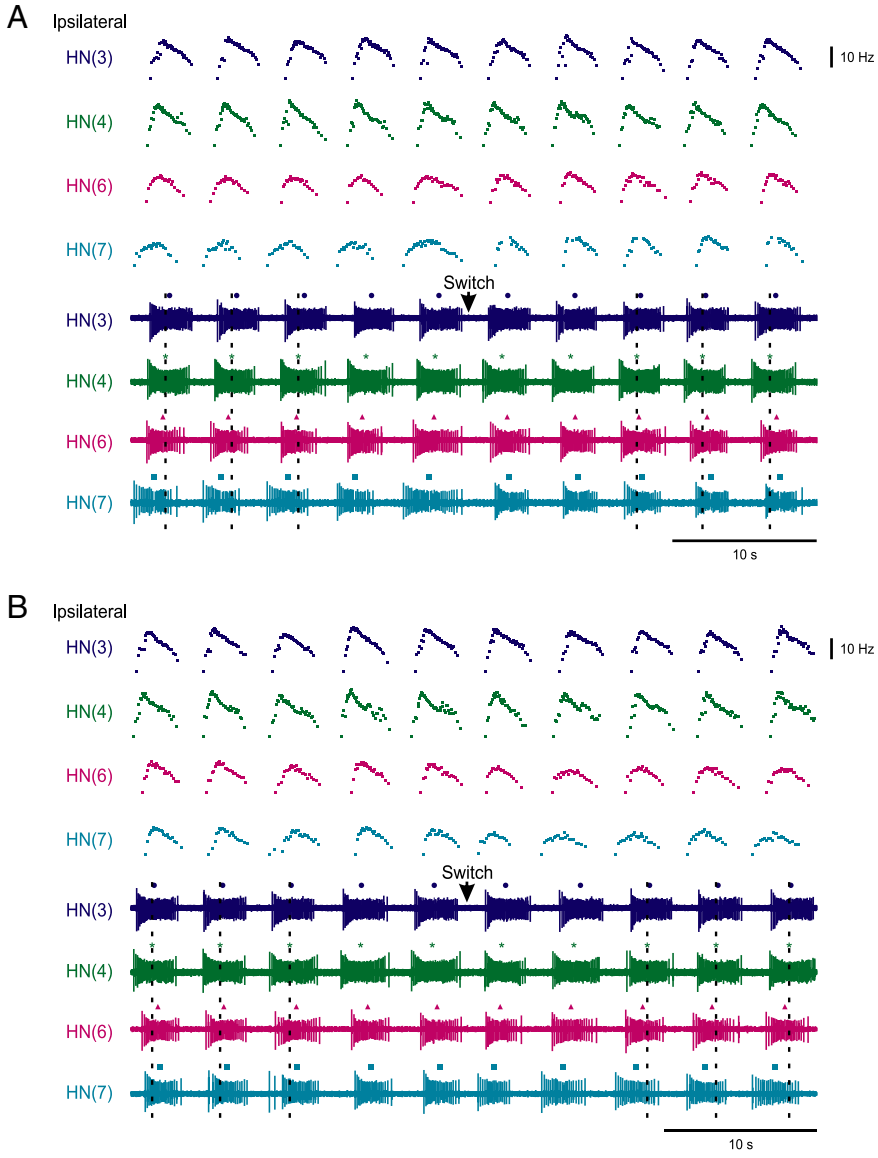


FIG. 2. Activity in all ipsilateral identified premotor interneurons heartbeat CPG during switches in coordination mode in a typical recording. *A*: switch from peristaltic to synchronous coordination mode. *B*: switch from synchronous to peristaltic coordination mode. *Top 4 traces*, *both panels*: instantaneous spike frequency plotted vs. time (all show largely decelerating bursts). *Bottom 4 traces*: extracellularly recorded *voltage traces*. Markers indicate the time of the median spike for each burst. Dashed vertical lines are centered on the median spike of several G4 interneuron bursts to ease comparison of relative (unilateral) phase during the 2 coordination modes. Switches are indicated with arrows. In this and all subsequent traces the heart interneuron (HN) recorded is indicated by color, midbody ganglion number (3–7 or X), and, if necessary, body side (L or R). Standard color and marker codes are applied in this and in all subsequent figures. See METHODS for color and marker codes.

where holding potential varied from −35 to −55 mV in an attempt to minimize escape spiking while maximizing IPSC amplitude). At the end of each experiment the electrode was withdrawn from the motor neuron and only data in which the electrode potential was within ±5 mV of ground were included. Thus holding potentials were accurate within ±5 mV.

For extracellular recordings from heart interneurons, we used suction electrodes filled with normal saline. Electrodes were pulled on a Flaming/Brown micropipette puller (P-97, Sutter Instruments, Novato, CA) from borosilicate glass (1 mm OD, 0.75 mm ID, A-M Systems, Carlsborg, WA) and placed in a suction electrode holder (E series, Warner Instruments, Hamden, CT). To ensure a tight fit between the cell and electrode, the electrode tips had a final inner diameter of about 20 $\mu$M, approximately the diameter of heart interneuron somata. The electrode tip was brought in contact with the cell body and light suction was applied using a syringe until the entire cell body was inside the electrode. Extracellular signals were monitored with a differential AC amplifier (model 1700, A-M Systems) at a gain of 1,000 with the low- and high-frequency cutoffs set at 100 and 1,000 Hz, respectively. Noise was reduced with a 60-Hz notch filter and a second amplifier (model 410, Brownlee Precision, Santa Clara, CA) amplified the signal appropriately for digitization.

### *Data acquisition and analysis*

Data were digitized (sampling rate ≥3.3 kHz) using a digitizing board (Digi-Data 1200 Series Interface, Axon Instruments, Foster City, CA) and acquired using pCLAMP software (Axon Instruments) on a personal computer (PC).

For analysis of extracellularly recorded spike trains to determine the heart interneuron activity pattern, spike detection was carried out in Spike2 (Cambridge Electronic Design, Cambridge, UK) using methods outlined previously (Masino and Calabrese 2002a,b). Briefly, spikes were detected with a discrimination window. When voltage crossed a lower threshold value, but did not exceed an upper threshold, a spike event was detected and was indicated by a raster point above the spike (Fig. 2*A*). The upper threshold eliminated transient artifacts in the recording. To prevent multiple detection of the same spike, a refractory period (20 ms), during which spikes could not be recognized, was applied after each detected event. To ensure that all spikes were detected, the refractory period was considerably shorter than the shortest interspike interval (about 50 ms).

In most recordings, heart interneuron spikes were easily discernable by eye because the only units present in the recording and the spike amplitude remained constant over periods of 20 min to ≥1 h. In a minority of the preparations, the extracellular recordings would lose

suction and have a signal that progressively grew weaker before the suction was reestablished. In these cases, the signal was low-pass filtered and differentiated to reduce noise levels relative to the signal. Then, spike thresholds were varied according to the differentiated signal levels.

For analysis of burst characteristics—period, duty cycle, and intraburst spike frequency—spikes were grouped into bursts as follows. After an interburst interval (1 s) elapsed without any spikes detected, the next spike event was identified as the first spike of a burst. Subsequent spikes with interspike intervals less than the interburst interval were grouped into that burst. To eliminate the effects of stray spikes in oscillator interneurons, groups of fewer than five spikes were not considered as bursts. The median spike in each burst was indicated by a symbol above the burst. In this paper, specific colors and specific symbols of the same color are used in traces, graphs, and diagrams to represent heart interneurons from specific midbody ganglia: red/diamond, G1/G2 interneurons; blue/circle, G3 interneurons; green/asterisk, G4 interneurons; orange/open circle, G5 interneurons; magenta/triangle, G6 interneurons; cyan/square, G7 interneurons; and lime green/cross, X interneurons.

We then calculated intraburst spike frequency, burst period ($T$), phase ($\phi$), and duty cycle ($D$) for each recorded cell. Every effort was made to maximize the number of representative bursts analyzed within a coordination mode. Bursts were not included if they were the result of injury, one to two cycles of disrupted patterning, or if one of the heart interneurons was no longer following 1:1 with the other heart interneurons. For this analysis 20.53 ± 1.10 (SD) cycles, on average, were used per preparation for each coordination mode with a minimum number of five cycles used (usually $n \geq 12$ consecutive bursts). In a few preparations, one or more heart interneurons were insufficiently inhibited (or "slightly damaged in the dissection and/or the recording") so that they continued to fire at very low rates (<5 Hz) during their inhibited phase. In this case, as few as possible detected spikes were removed around troughs in the instantaneous spike frequency to achieve a sufficient interburst interval (1 s) for burst detection. To represent the burst period of the entire central pattern generator the burst period of a G4 interneuron was determined.

The instantaneous spike frequency, defined as the inverse of the interval between consecutive spikes in a burst, was determined and used to calculate the maximum and the minimum spike frequency, and the mean spike frequency within each identified burst, which were then averaged across a series of bursts to yield the averages. Burst period was defined as the interval (in seconds) from median spike to median spike of consecutive bursts and burst period ($T_I$) of each cycle was determined for each cell with ganglionic index G($I$). These individual burst periods were then used to calculate the mean burst period for each cell. (The median spike was used for designating cycles because it leads to less cycle-to-cycle variation in period than either the first or the last spike.) The unilateral (or relative) phase of a given heart interneuron was defined on a cycle-by-cycle basis as the time ($t$) difference between its median spike ($t_I$) and the median spike of the ipsilateral G4 heart interneuron ($t_4$; unilateral phase marker cell). The time difference was then normalized to the burst period of the ipsilateral G4 heart interneuron and expressed as a percentage

$$\phi_I = \left(\frac{\Delta t_{I-4}}{T_4}\right) \times 100$$

A phase of 100/0% indicated a cell with no phase difference relative to the phase marker cell, whereas a 50% phase difference indicated an antiphasic relationship. To unify unilateral (relative) phase calculations in the two different modes or in bilateral recordings, the unilateral phase calculated in the synchronous coordination mode was offset by 51.1%, corresponding to the empirically measured phase difference (51.06 ± 2.16%; $n = 10$) in bilateral recording between the peristaltic G4 interneuron (defined as 0% phase) and the synchronous G4 interneuron (i.e., the peristaltic G4 interneuron became the absolute phase marker). Thus the absolute phase marker body side switches as the peristaltic side switches. This adjustment allowed a complete bilateral assessment of phase (absolute phase). A positive phase difference indicates a phase lag, whereas a negative phase difference indicates a phase lead with respect to the phase marker G4 heart interneuron (relative or absolute; unilateral or bilateral). Duty cycle ($D$) was defined as the fraction of the burst period occupied by the burst duration ($T_{burstI}$)

$$D = \left(\frac{T_{burstI}}{T_I}\right) \times 100$$

The mean duty cycle for each interneuron was then displayed as box plots (normalized burst duration) in the phase diagrams (Figs. 4 and 10, described below).

Bilateral phase diagrams were used to illustrate phase differences between heart interneurons (Figs. 4 and 10). The beginning and end of each box plot indicated the average time of the first and last spike, respectively, in a series of bursts relative to the median spike time of the absolute phase marker cell. Error bars indicated the SD around the mean first and last spikes in a burst. The average median spike time of the absolute phase marker cell [peristaltic HN(4) interneuron], indicated by a vertical line that bisected the phase box near its midpoint, was positioned at 100/0% phase on the diagram. The mean phase for each heart interneuron was plotted on the phase diagram with respect to the phase marker cell. Error bars indicated the SD around the averaged median spike in a burst. A shift of the average median spike to the right of 100/0% indicated a phase lag, whereas a shift of the average median spike time to the left of 100/0% indicated a phase lead.

A 2 × 6 (heart interneuron × coordination mode) factor multivariate ANOVA (MANOVA) was performed in SPSS (Chicago, IL) to test the significance of each dependent variable (i.e., phase, duty cycle, mean spike frequency, maximum spike frequency, and minimum spike frequency). Additional MANOVAs (Table 2*A*) were performed for each coordination mode separately to address relevant pairwise comparisons. Significant heart interneuron MANOVA differences ($P < 0.05$) were subjected to post hoc Tukey's honestly significant difference tests (Table 2, *B* and *C*). In a few cases, phase, duty cycle, and spike frequency outliers were removed to meet the assumptions of the MANOVA. Outliers were identified in SPSS as those values greater than or less than two times the interquartile range from the median.

We used an indirect method to identify the inhibitory postsynaptic currents (IPSCs) elicited by the unidentified heart interneuron [known to exist (Calabrese 1977) and referred to as the *X heart interneuron* or HN(X) neuron because its ganglionic index cannot be specified] and thus to determine its activity pattern. We analyzed data from 11 preparations in which switching was regular, with appropriate and robust changes in phasing of the interneuron X-mediated IPSCs across two to three switches or more. We recorded between two and 13 switches per preparation either in discontinuous current clamp or voltage clamp. Spike and IPSC detection was performed off-line using custom-made Matlab software (The MathWorks, Natick, MA) and pClamp analysis software in a multistep process. Spike times of the relevant premotor interneurons (G3 and/or G4) and the synaptic delay between their spike time and the time of the IPSCs in a G3 or G4 heart motor neuron were determined. These values were then used to identify, and graphically display, the IPSCs in the heart motor neuron caused by the known interneuron(s). All other postsynaptic potentials were attributed to the interneuron X. Next, the time of peak of each IPSC was determined using current traces that were filtered (low-pass, Gaussian) at 70—85 Hz for noise reduction. In each experiment, 11 to 13 bursts per coordination mode in each recorded heart motor neuron were analyzed. For interneuron X-mediated IPSC identification, events less than twice the size of the noise were rejected as were summed IPSCs. In seven of the 11 preparations, a G3 motor neuron

was recorded and in five a G4 motor neuron was recorded (i.e., in one preparation both motor neurons were recorded) but only the G3 motor neuron recordings were included in our summary phase, duty cycle, and intraburst spike frequency analysis to ensure uniformity of our X-mediated IPSC detection.

Spikes and IPSCs were then grouped into bursts. For spike trains the same criteria as described above were used. For bursts of IPSCs, we used 10% of the respective cycle period as the critical intraburst interval. Mean and maximum intraburst frequencies and duty cycles were calculated as described above for spike trains. The unilateral (relative) phase of the median IPSC of each IPSC burst, with respect to the median spike of the unilateral phase marker neuron's burst (the ipsilateral G3 or, in most cases, the ipsilateral G4 interneuron), and then the bilateral (absolute) phase were calculated as described above for spike trains. For the construction of phase diagrams, all phases in which the G3 interneuron was used as the unilateral phase marker were offset by +2.56% for the peristaltic mode and by +4.47% for the synchronous mode reflecting the averaged phase difference noted in the spike train analysis of premotor interneuron activity pattern (see Table 1). Results were analyzed statistically in conjunction with the data from the identified heart interneurons as described above.

## RESULTS

Our present aim was to characterize as quantitatively as possible the firing pattern of premotor heart interneurons in the heartbeat CPG. We recorded in isolated nerve cords from multiple preparations, to extract burst characteristics and phase relationships. Previous work has already provided such a quantitative description of the timing oscillator kernel of the CPG consisting of the first four pairs of heart interneurons (Hill et al. 2002; Masino and Calabrese 2002a,b). Here we ignore the coordinating interneurons of that kernel (heart interneurons of G1 and G2 whose activity with respect to the oscillator interneurons is now well characterized), which have no output to motor neurons, and focus on how the oscillator interneurons of G3 and G4 that do have outputs to motor neurons are coordinated with the rear premotor interneurons of G6 and G7. This coordination is mediated in part by the heart interneurons of G5, called *switch interneurons*, because switches in their activity state determine the two coordination modes of the heartbeat CPG, peristaltic and synchronous (Calabrese 1977; Gramoll et al. 1994; Lu et al. 1999). The phase relations in the timing core are not affected by such switches (Calabrese 1977) as will be extensively documented below. The G5 switch interneurons also control the activity of the unidentified heart interneuron pair of the CPG, the X interneurons (so designated because their ganglionic index cannot be specified in that their cell bodies have not been found) that have outputs to motor neurons (Calabrese 1977; Peterson and Calabrese 1982; Wenning and Calabrese 2005). After considering the identified interneurons we analyzed the activity pattern of the X heart interneurons, using indirect methods to extract their burst characteristics and phase relationships. Thus the characterization of the activity pattern of the heart interneuron in G3–G7, plus the X heart interneuron, presented here is as close an assessment of the output pattern of the heartbeat CPG as is presently possible. For the rest of the narrative below the front oscillator interneurons of G3 and G4 will be referred to often as a group as front premotor interneurons, the switch interneurons of G5 as switch interneurons, and the rear heart interneurons of G6 and G7 as rear premotor interneurons.

The recordings were always made with one reference oscillator interneuron, usually and preferably a G4 interneuron, which was chosen as the relative (unilateral) phase marker (see METHODS for how compensation was made, when a G4 interneuron was not recorded, or when recordings were bilateral), i.e., it was assigned a relative phase of 0% and phases of all other ipsilateral interneurons recorded were calculated with it as reference. [The G4 interneuron on the peristaltic side was chosen as the absolute (bilateral) phase marker, i.e., it was assigned an absolute phase of 0% and the G4 interneuron on the synchronous side was assigned an absolute phase of 51.1% as described in METHODS.] Typical recordings (Fig. 2) allowed unambiguous determination of the coordination modes and the switches between them. Only preparations where such lack of ambiguity was present were considered; preparations that produced ambiguous output patterns were usually associated with obvious injury to the preparation or were aged >2 h.

### *Identified premotor interneurons: activity pattern*

In total, 56 different preparations were recorded to determine the activity pattern of the identified premotor interneu-

TABLE 1. *Bilateral (absolute) phase, duty cycle, and intraburst spike frequency (mean, maximum, and minimum) for G3–G7 HN in both Peri and Sync coordination modes*

| | | | Intraburst Spike Frequency | | |
|---|---|---|---|---|---|
| Neuron | Phase | Duty Cycle | Mean | Maximum | Minimum |
| Peri HN(3) | 2.6 ± 6.7% | 59.0 ± 3.0% | 13.75 ± 2.59 | 20.02 ± 3.40 | 5.50 ± 0.79 |
| Peri HN(4) | 0.0% | 58.4 ± 2.5% | 14.17 ± 2.41 | 21.00 ± 3.80 | 5.73 ± 0.98 |
| Peri HN(6) | −10.7 ± 4.3% | 56.7 ± 4.4% | 12.90 ± 2.84 | 19.97 ± 4.25 | 4.22 ± 1.12 |
| Peri HN(7) | −19.8 ± 9.4% | 55.1 ± 5.9% | 11.84 ± 3.20 | 17.55 ± 4.96 | 4.21 ± 1.27 |
| Peri Contra HN(4) | 51.1 ± 2.2% | 55.8 ± 2.0% | 12.21 ± 1.60 | 17.65 ± 2.50 | 5.12 ± 0.85 |
| Sync HN(3) | 55.5 ± 6.9% | 59.3 ± 3.9% | 13.47 ± 2.45 | 19.63 ± 3.01 | 5.46 ± 0.98 |
| Sync HN(4) | 51.1% | 58.3 ± 3.0% | 13.96 ± 2.19 | 20.79 ± 3.58 | 5.60 ± 0.83 |
| Sync HN(5) | 17.4 ± 2.9% | 58.1 ± 6.1% | 10.99 ± 2.03 | 20.01 ± 2.79 | 3.89 ± 0.74 |
| Sync HN(6) | 57.8 ± 3.5% | 52.6 ± 3.8% | 14.33 ± 3.38 | 21.44 ± 4.95 | 5.54 ± 1.26 |
| Sync HN(7) | 58.1 ± 7.2% | 49.4 ± 5.3% | 12.91 ± 3.25 | 19.58 ± 4.71 | 4.88 ± 1.35 |
| Sync Contra HN(4) | 0.7 ± 1.4% | 57.0 ± 1.8% | 12.19 ± 1.25 | 18.03 ± 1.91 | 4.95 ± 0.67 |

Values are means ± SD. Data exclude the peristaltic G5 switch interneuron, which is in the silent state. The phase of the peristaltic G4 interneuron was fixed at 0.0% and that of the synchronous G4 interneuron at 51.06%. Included are recordings from 56 different preparations; in peristaltic mode 16 HN(3), 51 HN(4), 8 HN(5), 16 HN(6), and 39 HN(7) neurons were recorded, and in synchronous mode 17 HN(3), 44 HN(4), 17 HN(5), 17 HN(6), and 39 HN(7) neurons were recorded. See METHODS for details of phase calculations. HN, heart interneurons; Peri, peristaltic; Sync, synchronous.

rons (see Table 1 legend for details.). In Fig. 2, all the identified premotor interneurons are recorded in a single preparation. In Fig. 2*A* the preparation produces a pattern of activity, beginning from the rearmost interneuron and progressing forward, that is associated with peristaltic coordination; midrecord there is a switch and afterward near synchrony in the activity of all the interneurons indicates the synchronous coordination mode. In fact there is a small phase lag of the other premotor interneurons with respect to the G4 interneuron. Later in the same preparation (Fig. 2*B*), the preparation is clearly synchronous (again there is a small phase lag between the other premotor interneurons and the G4 interneuron) and at midrecord switches to the peristaltic coordination mode. The preparations used in these analyses all switched multiple times with apparent regularity (more than three times), although the regularity of the switching was not quantified. Rather the aim here was to make recordings that would allow quantitative assessment of the two patterns of activity and the role of the switch interneurons in those two patterns. Figure 2 also shows the spike frequency profiles of the interneurons in the two coordination modes. Such profiles were made for all recordings and, although it seems from visual inspection that the spike frequency profiles of the front premotor (oscillator) interneurons are more sharply defined than those of the rear premotor interneurons, consistent differences in spike frequency among the premotor interneurons across preparations or between coordination modes are less apparent and these were analyzed statistically below (Tables 1 and 2).

### *Identified premotor interneurons and the switch interneuron on the synchronous side: phase constancy*

An important property of many CPGs, especially those associated with locomotion, is *phase constancy*, where the phase relations and duty cycle of activity are invariant across changes in burst period. We have already noted that the motor neuron output pattern of the heartbeat CPG shows a form of phase constancy (Wenning et al. 2004b)—unconventional, in that the phase progressions involved are right–left asymmetric and do not progress regularly across segmental motor neurons. The output activity of the CPG shows this left–right asymmetry and nonuniform segmental phase progressions. Nevertheless, our hypothesis was that these phase relations and duty cycles would be invariant across changes in period. Here we also included recordings of the switch interneurons on the synchronous side (see following text for more details). The 56 preparations considered in this study naturally varied across a range of period from about 4.07 to 8.52 s (mean 5.9 ± 1.0 s) (Fig. 3). There were no significant correlations of phase or duty cycle across period in either the peristaltic or synchronous modes for any of the premotor interneurons and for the switch interneuron in its active state (synchronous coordination mode). Mean spike frequency did show some tendency to vary with period and significant correlations were noted for the G4 interneurons in both synchronous and peristaltic modes ($r = -0.465$, $P = 1.47 \times 10^{-3}$; $r = -0.415$, $P = 2.46 \times 10^{-3}$, respectively) and for the G7 interneuron in the synchronous mode ($r = -0.488$, $P = 1.64 \times 10^{-3}$). The regression lines for these relations have relatively shallow slopes [−0.96, −0.96, −1.56 Hz/s (mean spike frequency/average period), respectively], indicating small changes with period. Thus the heartbeat CPG output in terms of the identified premotor interneurons and the switch interneurons shows phase constancy. Previously we showed such phase constancy in the timing oscillator kernel (Masino and Calabrese 2002a,b).

### *Identified premotor interneurons and the switch interneuron on the synchronous side: phase and duty cycle relations*

This phase constancy allows us to combine the phase and duty cycle data across preparations and to produce a summary bilateral (absolute) phase diagram (Fig. 4) that provides a quantitative evaluation of the normal phase relations and duty cycles among the premotor interneurons in the heartbeat CPG. Significant differences in phase between a given interneuron and the ipsilateral G4 interneuron are noted as is the significant difference in phase between the two G4 interneurons: the synchronous and peristaltic phase diagrams were aligned by using bilateral recordings of the G4 interneuron ($n = 10$) where the peristaltic G4 interneuron served as the absolute (bilateral) phase marker and the synchronous G4 interneuron had an empirically determined bilateral phase of 51.06% (±2.16%) [i.e., all relative (unilateral) phases on the synchronous side were offset by 51.1%]. Theoretically this phase should be 50% because the reciprocally inhibitory G4 interneurons burst alternately. We performed a one-sample *t*-test to determine whether the observed phase was different from this theoretical value of 50%, and there was no statistical difference ($P = 0.153$, two-tailed test). Our method of representing the duty cycle of the different interneurons involves plotting the mean phase of the start of the burst (first spike), middle of the burst (median spike), and end of the burst (last spike) with their respective burst durations. The relative positions of these three points—start, middle, end—give an indication of the contour of the spike frequency profile of the neuron.

There are many important features of this summary diagram that should be emphasized with the help of Tables 1 and 2, which present numerical data on bilateral phase, duty cycle, and intraburst spike frequencies (mean, maximum, and minimum) (Table 1) and statistical analysis of differences (Table 2). First, on the peristaltic side, the rear premotor neurons are significantly earlier in their activity phase than both the front premotor interneurons, there is a small but not statistically significant phase lead of the G4 front premotor interneuron over the G3 front premotor interneuron, and the G7 rear premotor interneuron significantly leads the G6 premotor interneuron. These phase relations may be summarized by saying that there is a distinct front-to-rear phase progression in the firing of the premotor interneurons on the peristaltic side. The duty cycle of the G7 premotor interneuron is significantly shorter than that of both front premotor interneurons [although this difference is small; peristaltic: 55 ± 6 vs. 59 ± 3 (G3) and 58 ± 2% (G4); synchronous: 49 ± 5 vs. 59 ± 4 (G3) and 58 ± 3% (G4)]. Second, on the synchronous side, the rear premotor neurons are significantly later in their activity phase than G4 but not the G3 front premotor interneuron, there is a small statistically significant phase lead of the G4 front premotor interneuron over the G3 front premotor interneuron [55.5 ± 6.9 (G3) vs. 51.1% (G4)], and the G6 and G7 rear premotor interneurons are not significantly different in phase. These phase relations may be summarized by saying that there is near synchrony in the firing of the premotor interneurons on the

TABLE 2. *Summary statistics for Tables 1 and 3*

A

| Dependent Variable | Data Set: Both coordination modes: Neuron | Both coordination modes: Coordination mode | Both coordination modes: Neuron × coord. mode | Peristaltic neuron | Synchronous neuron |
|---|---|---|---|---|---|
| Phase | *** | *** | *** | *** | *** |
| Duty Cycle | *** | *** | *** | * | *** |
| Mean Spk Freq | *** | ** | * | *** | *** |
| Max Spk Freq | ** | n.s. | n.s. | ** | n.s. |
| Min Spk Freq | *** | ** | ** | *** | *** |

B

| Neuron | Comparison: Ipsilateral HN(4) Phase | Ipsilateral HN(4) DC | Ipsilateral HN(3) Phase | Ipsilateral HN(3) DC | Synchronous HN(5) Phase | Synchronous HN(5) DC | Contralateral neuron Phase | Contralateral neuron DC | HN(6) vs. HN(7) Phase | HN(6) vs. HN(7) DC |
|---|---|---|---|---|---|---|---|---|---|---|
| Peri HN(3) | n.s. | n.s. | | | | | *** | n.s. | | |
| Peri HN(4) | | | n.s. | n.s. | | | *** | n.s. | | |
| Peri HN(6) | *** | n.s. | *** | n.s. | *** | n.s. | *** | n.s. | *** | n.s. |
| Peri HN(7) | *** | * | *** | * | *** | n.s. | *** | *** | | |
| Peri HN(X) | *** | n.s. | *** | n.s. | n.s. | n.s. | n.s. | * | | |
| Sync HN(3) | * | n.s. | | | | | | | | |
| Sync HN(4) | | | * | n.s. | | | *** | n.s. | | |
| Sync HN(5) | *** | n.s. | *** | n.s. | | | | | | |
| Sync HN(6) | *** | *** | n.s. | *** | *** | * | | | n.s. | n.s. |
| Sync HN(7) | *** | *** | n.s. | *** | *** | *** | | | | |
| Sync HN(X) | *** | *** | *** | *** | n.s. | *** | | | | |

C

| Neuron | Comparison: Ipsilateral HN(4) Mean Spk Freq | Ipsilateral HN(4) Max Spk Freq | Ipsilateral HN(4) Min Spk Freq | Ipsilateral HN(3) Mean Spk Freq | Ipsilateral HN(3) Max Spk Freq | Ipsilateral HN(3) Min Spk Freq | Synchronous HN(5) Mean Spk Freq | Synchronous HN(5) Max Spk Freq | Synchronous HN(5) Min Spk Freq | Contralateral neuron Mean Spk Freq | Contralateral neuron Max Spk Freq | Contralateral neuron Min Spk Freq | HN(6) vs. HN(7) Mean Spk Freq | HN(6) vs. HN(7) Max Spk Freq | HN(6) vs. HN(7) Min Spk Freq |
|---|---|---|---|---|---|---|---|---|---|---|---|---|---|---|---|
| Peri HN(3) | n.s. | n.s. | n.s. | | | | | | | n.s. | | n.s. | | | |
| Peri HN(4) | | | | n.s. | n.s. | n.s. | | | | n.s. | | n.s. | | | |
| Peri HN(6) | n.s. | n.s. | *** | n.s. | n.s. | ** | n.s. | n.s. | n.s. | n.s. | | * | n.s. | n.s. | n.s. |
| Peri HN(7) | *** | ** | *** | n.s. | n.s. | *** | n.s. | n.s. | n.s. | n.s. | | n.s. | | | |
| Peri HN(X) | *** | | | *** | | | *** | | | n.s. | | | | | |
| Sync HN(3) | n.s. | | n.s. | | | | | | | | | | | | |
| Sync HN(4) | | | | n.s. | | n.s. | | | | n.s. | | n.s. | | | |
| Sync HN(5) | ** | | *** | n.s. | | *** | | | | | | | | | |
| Sync HN(6) | n.s. | | n.s. | n.s. | | n.s. | ** | | *** | | | | n.s. | | n.s. |
| Sync HN(7) | n.s. | | * | n.s. | | n.s. | n.s. | | * | | | | | | |
| Sync HN(X) | *** | | | *** | | | n.s. | | | | | | | | |

*A:* A 2 × 6 (Both Coordination Modes; heart interneuron × coordination mode) factor MANOVA was carried out on the data of Tables 1 and 3 for each dependent variable (i.e., phase, duty cycle, mean spike frequency, maximum spike frequency, and minimum spike frequency). Additional MANOVAs (Peristaltic and Synchronous) were performed for each coordination mode separately to enable specific pairwise comparisons. In the case of the X interneuron tests, data from Table 3 for the X interneuron alone were compared with the identified interneuron data in Table 1. *B:* Significant heart interneuron phase and duty cycle MANOVA differences ($P < 0.05$) were subjected to post hoc Tukey's honestly significant difference tests. Comparisons of the phase and duty cycle for each G3–G7 heart interneuron (HN) and the X heart interneuron recorded in both coordination modes—peristaltic (Peri) and synchronous (Sync)—(except the peristaltic G5 switch interneuron, which is in its silent state) with several other relevant heart interneurons were performed. These relevant neurons consist of the ipsilateral HN(4), the ipsilateral HN(3), the synchronous HN(5), each contralateral neuron, and the ipsilateral HN(6) versus HN(7). For the contralateral neuron tests, only the peristaltically coordinated neurons were tested against their contralateral homologs, except the synchronous G4 interneuron, which was also tested against its contralateral homolog. For the ipsilateral HN(6) versus HN(7) tests, the data are listed under the HN(6) row, although it is actually tested versus the ipsilateral HN(7). *C:* Post hoc Tukey's tests were also performed for significant MANOVA differences ($P < 0.05$) in the mean (Mean), maximum (Max), and minimum (Min) spike frequencies (Spk Freq) of each G3–G7 heart interneuron. Tukey's tests on each X heart interneuron were carried out only for the mean spike frequency because maximum and minimum spike frequencies were not measured. Comparisons were made with respect to the same neurons in *B*. Throughout the table significant differences are indicated by asterisks: $*P \leq 0.05$; $**P \leq 0.01$; $***P \leq 0.001$; nonsignificant test results are indicated by "n.s." If a test was not applicable or not justified by the MANOVA significance, the cell was left empty. The nominal $\alpha$-level for MANOVA and Tukey's test significance was 0.05.

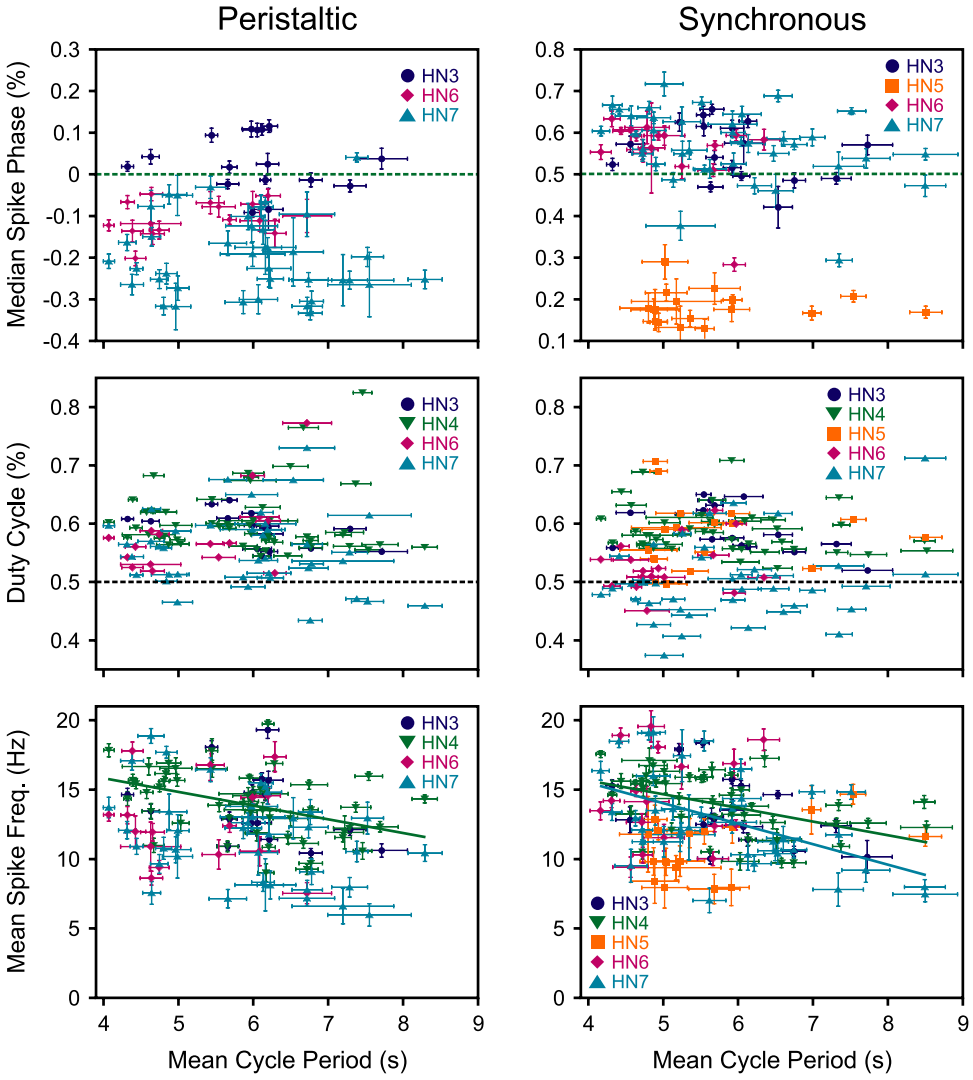


FIG. 3. Effect of burst period on heart interneuron phasing, duty cycle, and intraburst mean spike frequency. The Figure is broken up into 6 panels consisting of 2 columns for each coordination mode (peristaltic and synchronous, respectively) and 3 rows for the different firing properties (phase, duty cycle, and mean intraburst spike frequency, respectively). Each point in a graph consists of data averaged from one preparation and the error bars indicate SDs. *Duty cycle panels* do not have vertical error bars because they were calculated from subtraction of the average first burst spike phase from the average last burst spike phase. In the phase panels, green dashed line indicates the value of the phase of G4 heart interneuron with the peristaltic G4 interneuron assigned 0% phase (absolute phase marker) and the synchronous G4 interneuron phase determined from bilateral recordings to be 51.1% (see text for explanation). (See METHODS for how unilateral and absolute phases were calculated.) In the *duty cycle panels*, the black dashed line indicates 50% duty cycle. In all panels, statistical tests of the correlation of the data with burst period were carried out; only 3 tests were found to be significant (all in the mean spike frequency plots). These significant results are indicated by a fitted solid line of regression (specifically, the peristaltic G4 interneuron and the synchronous G4 and G7 interneurons).

synchronous side but the G4 front premotor interneuron slightly leads the others in phase. The duty cycle of both the G6 and G7 rear premotor interneurons is significantly shorter than that of both the G3 and the G4 front premotor interneurons and the G7 rear premotor interneuron has a significantly shorter duty cycle than the G6 rear premotor interneuron. Third, all side-to-side differences in phase between premotor interneurons from the same segmental ganglion are statistically significant. On the synchronous side the duty cycle of the rear premotor neurons is significantly shorter than that of their segmental homologs on the peristaltic side.

### *Identified premotor interneurons and the switch interneuron on the synchronous side: spike frequency characteristics*

We compared the spike frequency characteristics for the premotor (and synchronous switch) interneurons by analyzing the maximum, minimum, and mean spike frequencies for each interneuron (Tables 1 and 2*C*). Significant differences were found for the rear premotor interneurons with respect to the G4 front premotor interneuron on the peristaltic and, to a lesser extent, the synchronous side. There is thus some tendency for the rear premotor interneurons to burst a bit more weakly than the front premotor interneurons.

### *Switch interneurons: activity pattern and phase and burst characteristics*

In eight of the 56 preparations, we recorded a switch interneuron in conjunction with an ipsilateral G4 interneuron (front premotor interneuron) and one or more rear premotor interneurons, during both coordination modes. These preparations allowed us to determine whether indeed the synchronous coordination mode was associated with the active and the peristaltic coordination modes with the silent state of the switch interneuron and whether switches in coordination mode of the premotor interneurons were always associated with switches in the activity state of the switch interneurons. Figure 5*A* shows a typical switch from peristaltic to synchronous coordination. At the beginning of the record the premotor interneurons are coordinated peristaltically and the switch interneuron is in its silent state. With the extracellular recording technique used here, we often noticed a low level of spike activity in the switch interneuron in its silent state. Such low-level activity has been noted previously in intracellular recordings but was assumed to be a result of injury (Calabrese 1977; Gramoll et al. 1994; Lu et al. 1999). Here we assume that the activity is not caused by injury and reflects a lack of complete suppression of spike activity. Thus the silent state of the switch interneuron

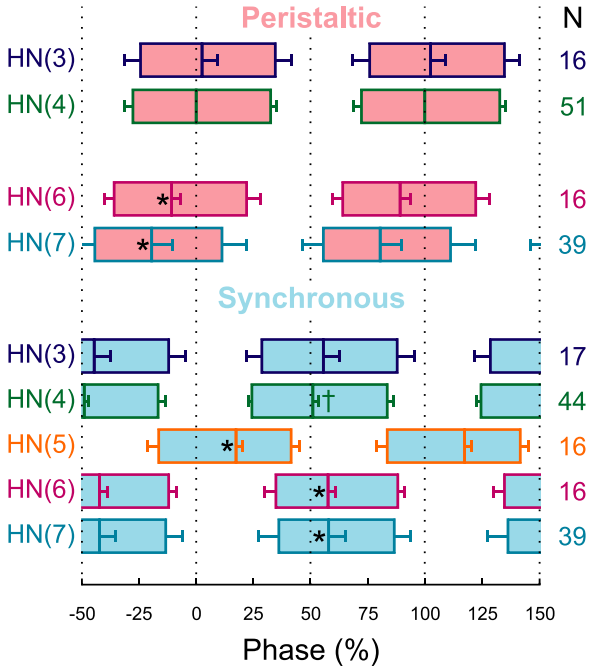


FIG. 4. Summary bilateral phase diagram of the premotor and switch interneurons of the heartbeat central pattern generator. A unilateral phase diagram was constructed with measurements of activity phase relative to the ipsilateral G4 interneuron's median spike as described in METHODS for both synchronous and peristaltic coordination modes. Average (mean) duty cycle is indicated by the length of the bar. To align the unilateral phase diagrams into a bilateral diagram the phase of the synchronous G4 (indicated by a cross) was measured with respect to the peristaltic G4 interneuron in bilateral recordings (51.06 ± 2.16%). All other synchronous measurements were then offset by 51.1% (i.e., the same amount as the phase of the synchronous G4 interneuron). Synchronous coordination is indicated by sky blue and peristaltic coordination by hot pink. *Left edge* of each bar indicates the average phase of the first spike of the burst; *right edge* indicates the average phase of the last spike of the burst. Average phase is indicated by a vertical line within the bar. Relative positions of these 3 points—start, middle, end—give an indication of the contour of the frequency profile of the neuron. Error bars indicate SDs. MANOVAs and Tukey's post hoc tests were carried out to compare the phase of each interneuron with its ipsilateral G4 phase marker. Significant differences in phase with respect to the ipsilateral G4 interneuron are indicated by a single asterisk (Table 2*B*).

can show rudimentary activity. At midrecord the switch interneuron suddenly enters its active state and the premotor interneurons rapidly switch to being coordinated synchronously. Figure 5*B* shows the typical activity pattern when the switch interneuron is in its active state, including spike frequency profiles for the front and rear premotor interneurons and the switch interneuron. The switch interneuron has a distinctly different spike frequency profile in which spike frequency accelerates as the burst progresses, unlike that of the premotor interneurons where spike frequency declines as the burst progresses. This spike frequency profile was previously noted in intracellular recordings (Gramoll et al. 1994; Lu et al. 1999) and was observed in all our extracellular recordings here. Figure 5*C* shows a typical switch from synchronous to peri-

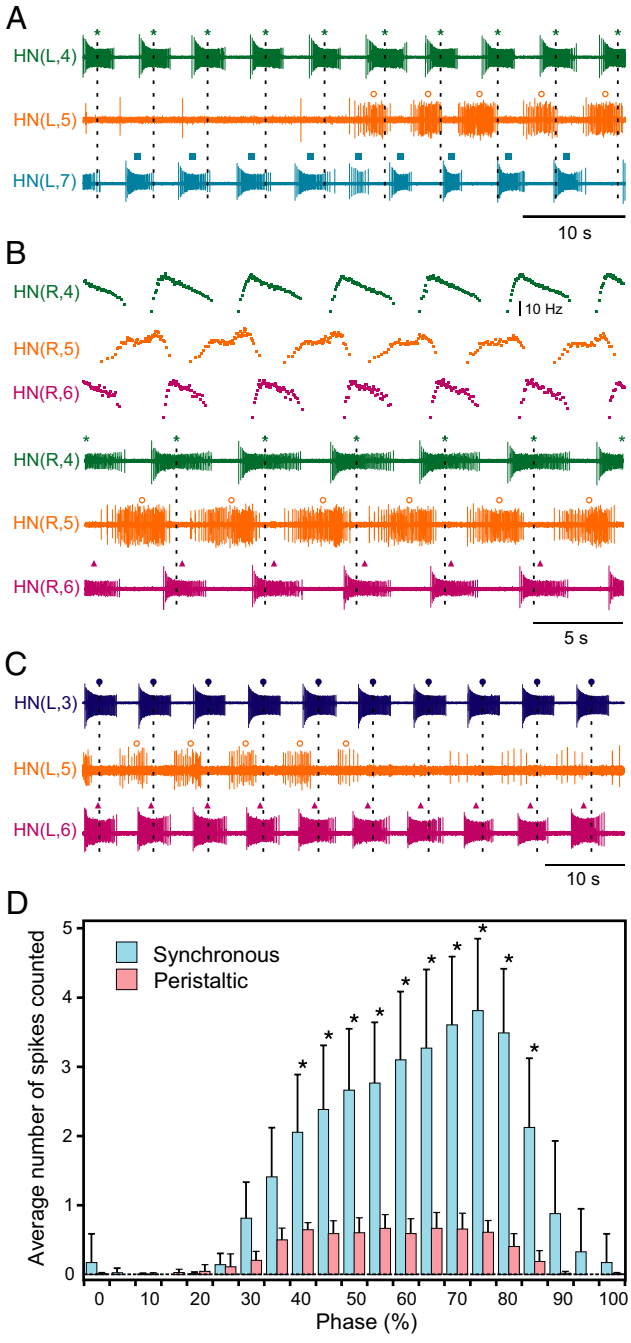


FIG. 5. Activity state, burst characteristics, and phase of the switch interneuron (G5 interneuron) during both coordination modes of the heartbeat CPG and during switches in coordination mode. *A*: switch from peristaltic to synchronous coordination mode. *B*: typical switch interneuron activity during synchronous coordination mode. Notice the characteristic accelerating burst profile of the switch interneuron in synchronous mode. *C*: switch from synchronous to peristaltic coordination mode. In *A*, *B*, and *C*, 3 *extracellular voltage traces* are shown. Standard markers indicate the time of the median spike for each burst. Vertical lines are centered on the unilateral phase marker (G3 or G4) interneuron's median spike to ease visualization of relative phasing. In *B*, 3 instantaneous spike frequency plots are shown above their corresponding *extracellular voltage traces* shown below. *D*: comparison of phasing and burst characteristics of the switch interneuron in both coordination modes; phase is relative (unilateral), albeit for peristaltic mode absolute and relative phases are the same. Average phase histograms (5% phase bins) were constructed for each experiment in both coordination modes. For each experiment the average number of spikes per phase bin was calculated by dividing the total count of spikes within a bin by the number of bursts counted. These data were averaged across experiments ($n = 8$) in both modes; error bars indicate SDs. Note there are no changes in the relative phase of the switch interneuron across switches. Paired *t*-tests were carried out to look for significant differences between the 2 modes in each phase bin. Nominal $\alpha$-level was 0.05. Because of the multiple ($n = 20$) comparisons, the Dunn–Šidák-compensated $\alpha$-level was $2.56 \times 10^{-3}$. Significant differences are indicated by an asterisk.

staltic coordination. At the beginning of the record the premotor interneurons are coordinated synchronously and the switch interneuron is in its active state. At midrecord the switch interneuron suddenly enters its silent state (activity is dramatically reduced and bursts no longer accelerate) and the premotor interneurons rapidly switch to being coordinated peristaltically. Note that in both switches (Fig. 5, *A* and *C*) the change in coordination is made by a change in the rear premotor interneuron's activity pattern; the front premotor interneuron apparently is not perturbed by the switch.

Across the eight preparations we averaged the number of spikes in the switch interneuron in the peristaltic and synchronous coordination modes of the premotor interneurons in 5% phase bins (Fig. 5*D*). The synchronous mode is associated with robust accelerating bursting in the switch interneurons and the peristaltic mode with weak firing in the switch interneuron. Significantly, the switch interneuron activity occurs at the same phase with respect to the ipsilateral G4 interneuron in both coordination modes (corresponding to relative phase)—thus the switch interneurons are in antiphase on the two sides (absolute phase). Like the front premotor interneurons the activity phase for the switch interneurons is fixed, whereas those of the rear premotor interneurons change across a switch. This latter point is emphasized in the two switches shown in Fig. 6. In these cases a bilateral pair of rear premotor interneurons is recorded. One sees that a change in the activity state of the switch interneurons is associated with a change in the phase of the ipsilateral rear premotor interneuron with respect to the front premotor interneuron and a corresponding change in the side-to-side phase difference between the bilateral rear premotor interneurons. This side-to-side change implies a reciprocal switch in the activity state of the contralateral (not recorded) switch interneuron.

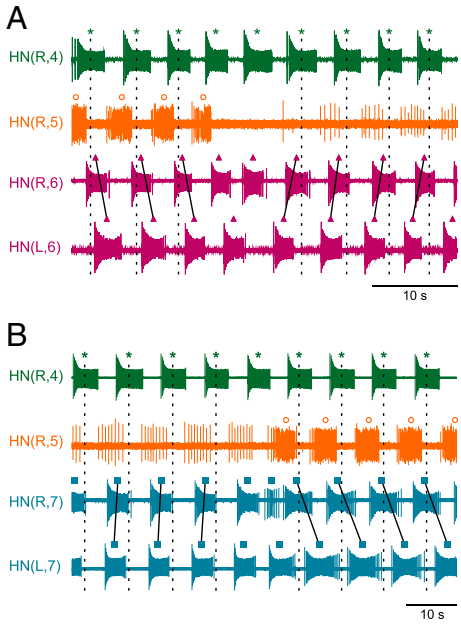


FIG. 6. Direct demonstration that switches in switch interneuron activity state are associated with bilateral changes in coordination mode. *A*: a switch from right side synchronous to right side peristaltic coordination mode, while recording G4 heart interneuron (as the phase marker), the right G5 switch interneuron, and bilaterally from the two G6 rear premotor interneurons. *B*: switch from right side peristaltic to right side synchronous coordination mode, while recording the right G4 heart interneuron (as the phase marker), the right G5 switch interneuron, and bilaterally from the two G7 rear premotor interneurons. In *A* and *B* recordings are extracellular and standard markers indicate the time of the median spike for each burst. Dashed vertical lines are centered on the median spike of several G4 interneuron bursts to ease determination of coordination mode. Solid lines are drawn between the median spike markers of adjacent full burst of the two rear premotor interneurons to show the bilateral shift in the rear premotor interneurons' coordination. Note that the bilateral switches in coordination mode are associated with a switch in the activity state of the switch interneuron.

The summary bilateral phase diagram of Fig. 4, derived mainly from ipsilateral recordings, indicates that in each case the synchronous rear premotor interneuron should lead in phase its contralateral homologue and this prediction is borne out by these bilateral recordings. The phase and duty cycle of the synchronous switch interneuron's activity are also summarized in Fig. 4. This neuron fires in rough antiphase to all the rear premotor interneurons bilaterally and with the front premotor interneurons ipsilaterally.

### *Identified premotor interneurons and the switch interneuron on the synchronous side: variability in duty cycle and phase among preparations*

An important aspect of this quantitative description is an assessment of the variability in the CPG's activity. We assessed this variability by making histograms of bilateral (absolute) phase and duty cycle for all the premotor interneurons and for the switch interneuron on the synchronous side (i.e., in its active state) (Fig. 7). Because the G4 front premotor interneuron on the peristaltic side was used as the bilateral phase marker its phase variability could not be assessed. What is obvious from this analysis is that the G7 rear premotor interneuron is the most variable in both phase and duty cycle in both coordination modes; in the peristaltic mode the distribution of phases appears bimodal. The variability in phase is especially large and suggests that the G7 interneurons are least tightly bound within the pattern generator. Another aspect of this analysis that deserves mention is that the phase of the G3 front premotor interneuron is quite variable on both sides. This variability derives from a minority of preparations where the G3 interneuron in both the peristaltic and synchronous coordination mode leads the ipsilateral G4 interneuron in phase, giving a bimodal shape to the distribution. This tendency for a minority of preparations to show a phase lead of the G3 interneuron over the ipsilateral G4 interneuron was noted before and that analysis suggests that in these cases the G3 interneuron pair has a faster inherent period than that of the G4 interneuron pair, whereas in most preparations the reverse is true (Hill et al. 2002; Masino and Calabrese 2002a,b). The functional significance of the bimodality is not clear at this time.

### *The unidentified premotor X interneurons: phase, duty cycle, and spike frequency*

In seven additional preparations to those described above, we indirectly measured the activity of the unidentified X interneurons by recording the synaptic currents in known postsynaptic targets. The X interneurons are defined by their input to heart motor neurons in G3–G6 on both peristaltic and synchronous sides, and their electrical coupling to ipsilateral G3 and G4 heart interneurons (Fig. 8) (Calabrese 1977). These

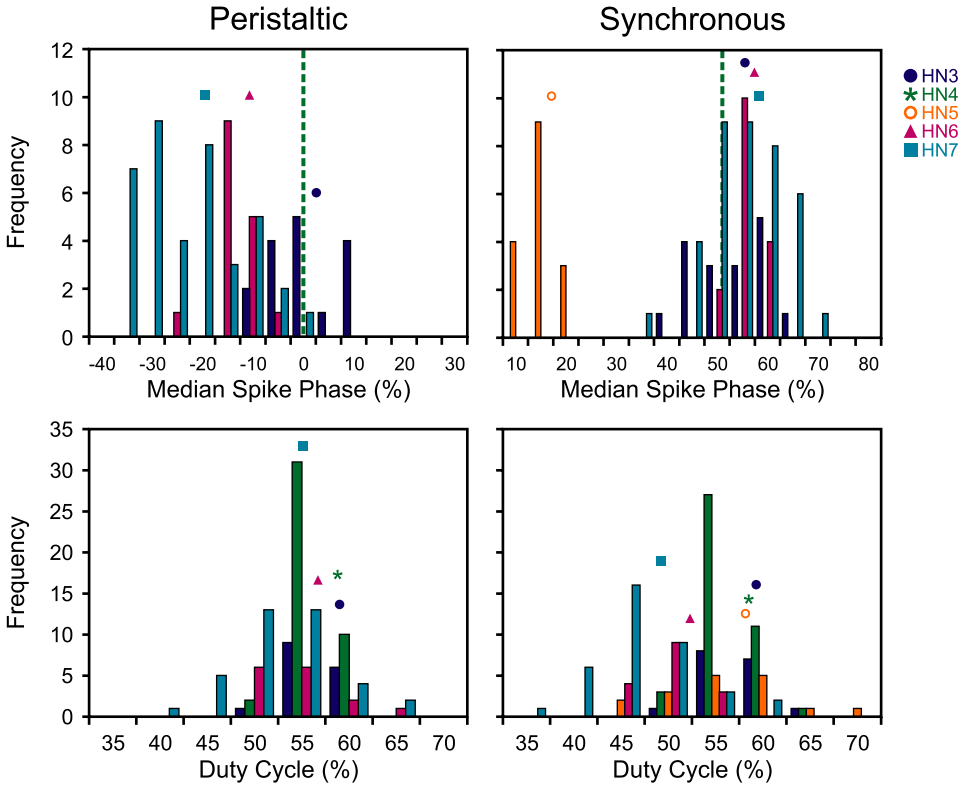


FIG. 7. Variability in phasing and duty cycle across preparations. The figure is broken up into 4 panels consisting of 2 columns for each coordination mode (peristaltic and synchronous, respectively) and 2 rows for the different firing properties (phase and duty cycle, respectively). Standard marker type and color were used throughout the figure. Markers indicate roughly the average for comparison with the distributions. Green vertical line indicates the value of the absolute phase of the G4 interneuron, the phase marker by which all other measurements were made. With the exception of the G7 interneuron's peristaltic phase, most distributions appear to be roughly normal and relatively tight.

X-mediated IPSCs are strong in the motor neurons of G3 and G4; moreover only the ipsilateral (Fig. 8*A*) G3 premotor interneuron connects to these motor neurons. Thus by recording the G3 interneuron and an ipsilateral G3 or G4 motor neuron unambiguously one can assign all IPSCs mediated by the G3 interneuron and thus by "subtraction" determine the IPSCs mediated by the X interneuron and thus its firing pattern. This method is illustrated in Fig. 9, *A* and *B*. Only recordings of G3 motor neurons are included here ($n = 7$), but similar results were obtained from recordings in the G4 motor neurons ($n = 5$, data not shown). Across the seven preparations where we assessed the X premotor interneuron–mediated IPSCs in the G3 motor neuron we averaged the number of spikes in the X interneuron in the peristaltic and synchronous coordination modes (11–13 bursts per mode) of the premotor interneurons in 5% phase bins (Fig. 9*C*). We then assessed duty cycle and mean intraburst spike frequency as we did for the identified premotor and switch interneurons. These may be regarded as underestimates because our procedure may have missed small X-mediated IPSCs, especially at the beginning and end of the IPSC burst. Relative phase was assigned with respect to the ipsilateral G4 interneuron when recorded ($n = 4$) or the ipsilateral G3 interneuron (always recorded) ($n = 3$). If assigned with respect to the G3 interneuron it was corrected to the G4 interneuron by offsetting by 2.6% in the peristaltic and by 4.5% in the synchronous coordination mode as in the summary bilateral (absolute) phase diagram of Fig. 4. Absolute phase was then calculated by assigning the peristaltic G4 interneuron a phase of 0% and the synchronous G4 interneuron a phase of 51.1% as in the summary phase diagram of Fig. 4 (i.e., the relative phases on the synchronous side were all offset by 51.1%). G4 interneuron burst characteristic and phase were assessed as in Fig. 4 and Table 1. Summary data in this analysis

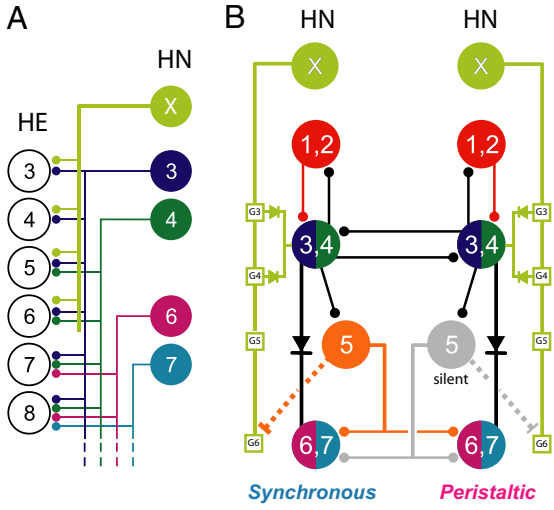


FIG. 8. Network diagrams for the leech heartbeat CPG and associated heart motor neurons including the X interneuron. *A*: hemilateral circuit of premotor interneurons (HN) of the CPG and their pattern of synaptic connections to motor neurons (HE) in G3–G8. *B*: circuit diagram showing synaptic connections among interneurons of the heartbeat CPG. In both panels, large colored circles are cell bodies and associated input processes. Lines indicate cell processes, small colored/black circles indicate inhibitory chemical synapses, small boxes along the X interneurons' axons in G3–G6 are putative spike initiation sites, and diodes indicate rectifying electrical synapses. Dashed process extending from the G5 interneuron to the G6 initiation site of the X interneuron indicates the indirect excitatory pathway explored in Figs. 11 and 12. For simplicity in the CPG diagram of *B* cells with similar input and output, connections and function are lumped. Standard colors for the identified interneurons are used; e.g., lime green is used for the X interneuron, which is defined as one that gives rise to matched inhibitory postsynaptic potentials (IPSPs) in ipsilateral G3–G6 heart motor neurons and rectifying electrical coupling potentials in ipsilateral G3 and G4 interneurons (Calabrese 1977).

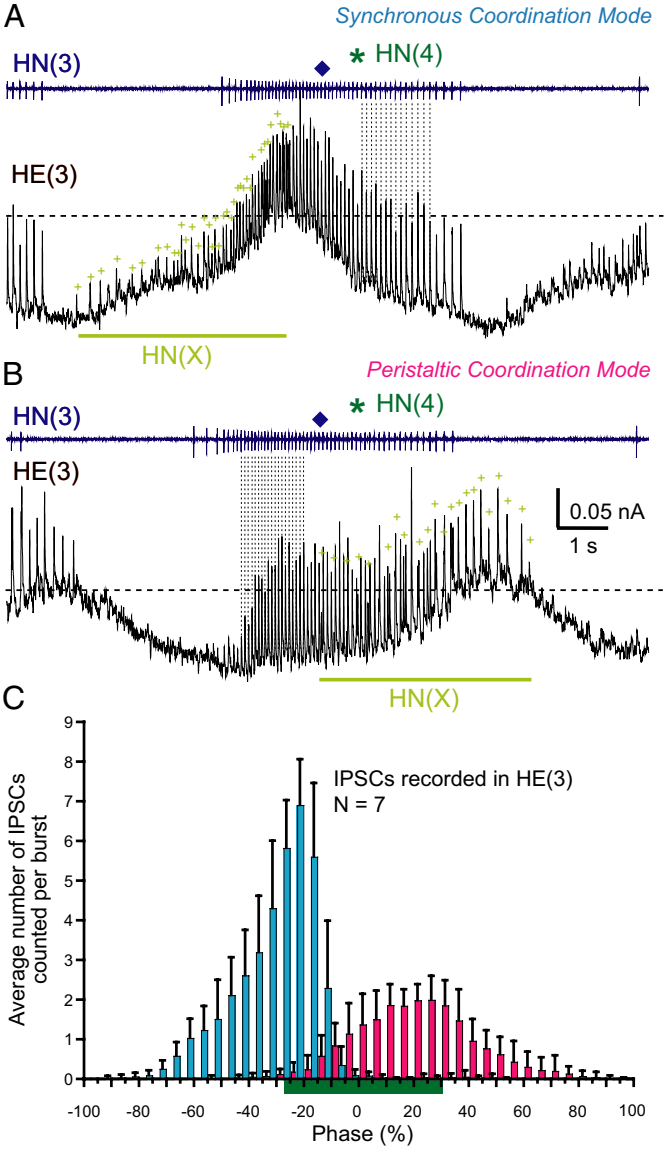


FIG. 9. Detecting the IPSCs in the G3 heart motor neuron and establishing the unilateral phase, duty cycle, and intraburst spike frequency for the X interneuron "burst." *A* and *B*: bursts of IPSCs recorded under voltage clamp in a G3 motor neuron in the synchronous and peristaltic coordination modes. Data from the experiment of Fig. 11 (holding potential: −56 mV; dashed lines indicate 0-nA holding current). In this experiment, spike activity was recorded extracellularly in ipsilateral G3, G4, and G5 interneurons. Spikes of the ipsilateral G3 interneuron (shown) were used to identify G3 interneuron-mediated IPSCs in the G3 motor neuron (vertical dashed lines indicate some of these identified IPSCs). Remaining unidentified IPSCs (meeting criteria outlined in METHODS) were ascribed to the ipsilateral X interneuron (lime green cross marker). Burst durations of the X-mediated IPSCs are indicated by a lime green bar. Recording is centered on the median spike of the ipsilateral G4 interneuron (green asterisk). Note the different unilateral phase of the X-mediated IPSCs with respect to the G3 interneuron's burst in the 2 coordination modes. *C*: displayed is the mean number of IPSCs per burst (±SD) averaged >11–13 bursts per coordination mode in 5% phase bins for all 7 experiments when a G3 motor neuron was recorded. Green bar: duty cycle of the ipsilateral G4 premotor interneuron with the median spike at 0% phase. These averaged results were used to generate the bilateral phase diagram of Fig. 10. Note that there are more X-mediated IPSCs in the synchronous than in the peristaltic coordination mode, and that X-mediated IPSC frequency is accelerating during a "burst" in the synchronous mode.

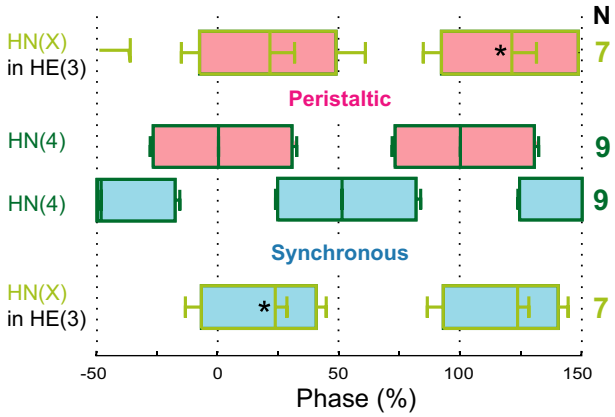


FIG. 10. Summary bilateral phase diagram of the X-mediated IPCSs recorded in the G3 heart motor neuron [HE(3)] in relation to the G4 interneuron [HN(4)] in both coordination modes. A unilateral phase diagram was constructed with measurements of X-mediated IPSC phase relative to the ipsilateral G4 interneuron's median spike, as described in METHODS and illustrated in Fig. 9, for both synchronous and peristaltic coordination modes. To align the unilateral phase diagrams into a bilateral diagram the phase of the synchronous G4 interneuron was assigned a phase of 51.1% (see Fig. 4 and METHODS) and phases of the synchronous X-mediated IPSCs were then offset by the same amount. Synchronous coordination is indicated by sky blue and peristaltic coordination by hot pink. Duty cycles are represented by plotting the mean phase of the start of the burst (first spike or IPSC), middle of the burst (middle spike or IPSC), and end of the burst (last spike or IPSC) with their respective burst durations. MANOVAs and Tukey's post hoc tests were carried out to compare the phase of each interneuron with its ipsilateral G4 interneuron (unilateral phase marker cell). Significant differences in phase with respect to the ipsilateral G4 interneuron are indicated by a single asterisk (Table 2*B*).

are presented in Fig. 10 and Table 3, and statistical comparisons of phase, duty cycle, and mean intraburst spike frequency for the X interneuron with the data set of Table 1 are included in Table 2.

The synchronous mode in the X interneurons is associated with robust accelerating bursting at a mean frequency about twice as high as that observed in the peristaltic mode (8.5 ± 1.3 vs. 3.85 ± 0.5 Hz) (see also Fig. 9 and Table 3), albeit MANOVA did justify contralateral comparison (Table 2*C*). Duty cycle in the X interneuron is significantly longer in the peristaltic than in the synchronous coordination mode (51.8 ± 9 vs. 47.0 ± 6.1%) (Table 2*B*), although the difference is small. Significantly, the X interneuron activity occurs at a very different phase with respect to the ipsilateral G4 interneuron

TABLE 3. *Bilateral (absolute) phase, duty cycle, and mean intraburst spike frequency for G4 and X HN in both Peri and Sync coordination modes*

| Neuron | Phase | Duty Cycle | Mean Spike Frequency |
|---|---|---|---|
| Peri HN(X) | 21.6 ± 9.1% | 51.8 ± 9.0% | 3.85 ± 0.51 |
| Sync HN(X) | 23.0 ± 4.8% | 47.0 ± 6.1% | 8.49 ± 1.28 |
| Peri HN(4) | 0.0% | 57.8 ± 2.2% | 14.17 ± 2.41 |
| Sync HN(4) | 51.1% | 57.3 ± 1.5% | 13.96 ± 2.19 |

Values are means ± SD. The phase of the peristaltic G4 interneuron was fixed at 0.0% and that of the synchronous G4 interneuron at 51.06%. The data on the X interneuron phase, duty cycle, and mean intraburst spike frequency were incorporated in the statistical analysis of table 2. No data from the G4 interneuron were included in that analysis; the G4 interneuron was used solely as a phase marker for the X interneuron. Data are from seven different preparations in which X-mediated IPSCs in a G3 motor neuron were recorded. See METHODS. See Table 1 for abbreviations.

(relative phase) in the two coordination modes [nearly antiphase on the synchronous side and nearly in phase on the peristaltic side (Fig. 9; see also Fig. 11)]—thus the X interneurons are roughly in phase on the two sides: 21.6 ± 9.1 peristaltic versus 23.0 ± 4.8 synchronous and the small difference is not statistically different (Table 2*B*). These phase relations expressed in absolute phase are summarized with respect to the G4 interneurons in the bilateral phase diagram of Fig. 10.

### *The unidentified premotor X interneurons: relation to the switch interneuron*

In two of the seven preparations, we simultaneously recorded the switch interneuron and identified X-mediated IPSCs in a G3 or a G4 heart motor neuron across six and nine switches, respectively. The active (synchronous) state of the switch interneuron was associated with the synchronous pattern of X-mediated IPSCs and the inactive state with the peristaltic pattern. This correlated transition in activity states of the switch interneurons and the X interneurons is apparent in the recordings in both coordination modes and across a switch from the peristaltic to the synchronous coordination mode in the records of Fig. 11. Note in the switch of Fig. 11*B* that the X-mediated IPSCs come into phase with the switch interneuron when it enters its active state (continuing in the synchronous coordination mode recording of Fig. 11*C*). The similarity in the burst pattern of the synchronous switch interneuron and the IPSC pattern of the synchronous X interneuron (Fig. 11, *B* and *C*) invited a correlation of switch interneurons spikes and synchronous X-mediated IPSCs. During the latter half of the synchronous switch interneuron burst there is a strong correlation of spikes and IPSCs matched by hand (see METHODS) (Fig. 12*A*) and this is also apparent in a spike-triggered average in which roughly the last 30 of a total of about 50 spikes in the synchronous switch interneuron's bursts were used (i.e., the first 20 spikes in the bursts were discarded) (Fig. 12*B*). Similar spike-triggered average IPSCs were observed throughout bursts of the switch interneurons that were smaller in amplitude but similar in temporal dispersion (half-width). The latency of the IPSCs is very long (193.5 ms) between spikes in the switch interneuron HN(5) to IPSCs in the G3 motor neuron HE(3), indicating an indirect interaction. Similar results were obtained in the second preparation. Here the latency was 164.2 ms between spikes in the switch interneuron HN(5) to IPSCs in the G4 motor neuron HE(4). Such temporal associations were previously observed and interpreted as indicating that X interneuron spikes arise in response to excitatory drive from the switch interneuron at a rear initiation site in its axon and travel frontward; in the peristaltic mode the direction of travel of X interneurons spikes appears rearward and these spikes are not excited by the switch interneuron (Calabrese 1977; Thompson and Stent 1976b,c) (Fig. 8*B*). Moreover, it was shown earlier that driving spikes in a switch interneuron with injected current pulses drives "X-mediated" IPSPs in ipsilateral front heart motor neurons (see Fig. 9 of Peterson and Calabrese 1982).

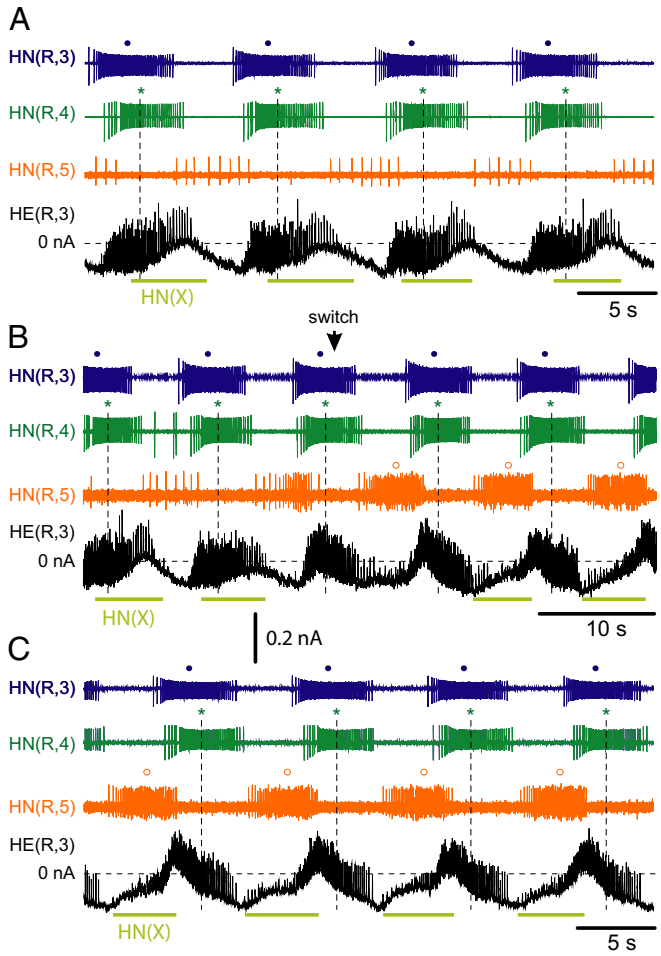


FIG. 11. Demonstration that switches in switch interneuron activity state are associated with changes in the X-mediated IPSC pattern coordination. All recordings are on the *right* side. *A*: recording in peristaltic coordination mode. *B*: switch from peristaltic to synchronous coordination mode. *C*: recording in synchronous coordination mode. In *A*, *B*, and *C*, ipsilateral recordings of X-mediated IPSCs in the G3 motor neuron (voltage clamp), and spike activity (extracellular recording) in the G3 interneuron, in the G4 heart interneuron (unilateral phase marker), and in the G5 switch interneuron are shown. Holding potential was −56 mV. Standard markers indicate the time of the median spike for each burst. Burst durations of the X-mediated IPSCs are indicated by lime green bars below the G3 motor neuron *current trace*. Note the shift in X-mediated IPSC coordination across the switch in activity state of the switch interneuron. Dashed vertical lines are centered on the median spike of the G4 interneuron bursts to ease determination of coordination mode.

## DISCUSSION

What general insights can be extracted from a quantitative description of the activity pattern of the interneurons constituting a central pattern generator such as we have attempted here?

### *Functional dissection of a central pattern generator*

In the leech heartbeat central pattern generator, beat rhythm and intersegmental premotor pattern can be conceptually separated. The first four pairs of interneurons compose a basic timing network with "fixed" side-to-side phase relations that set the basic rhythm corresponding to the regular bursting of heart motor neurons and beating of the hearts (beat rhythm generator) (Masino and Calabrese 2002a). This beat rhythm generator is then connected to the rear interneurons indirectly through the switch interneurons bilaterally and directly through ipsilateral electrical coupling. These connections link the identified premotor interneurons together (Fig. 1). The switch

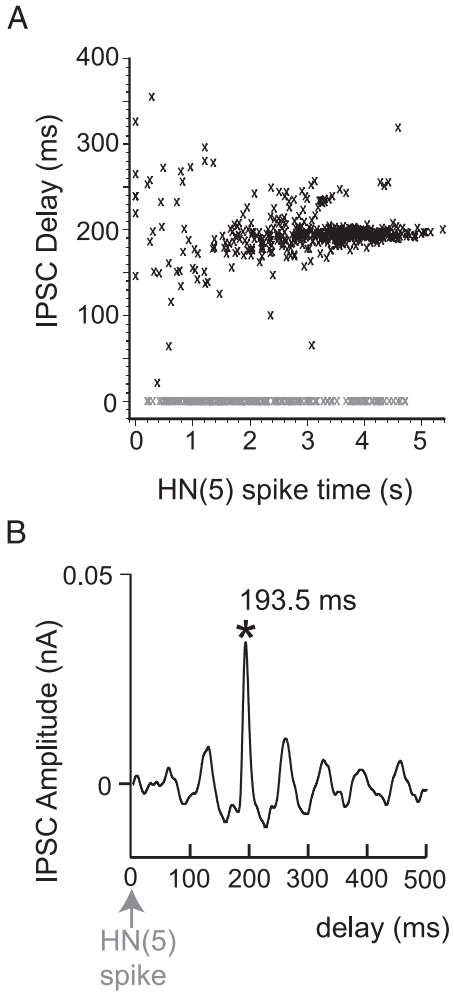


FIG. 12. Analysis of the relation between X-mediated IPSCs and spikes recorded in the G5 switch interneuron [HN(5)]. *A*: spikes recorded in the switch interneuron are associated with X-mediated IPSCs in the G3 motor neuron in the synchronous coordination mode. Relation between spikes in the switch interneuron and X-mediated IPSCs in the motor neuron was assessed by plotting the interneuron spike times vs. the IPSCs (12 bursts). Time was set to 0 for the first spike in each G5 interneuron burst. A total of 631 spikes were recorded and 422 X-mediated IPSCs identified (see METHODS). For 221 spikes no X-mediated IPSCs were identified (green × symbols). A total of 9 (i.e., on average less than one per G5 interneuron burst) X-mediated IPSCs were identified (≥200 ms) before the first spike in the G5 switch interneuron was recorded. Temporal association improves in the second half of the burst. *B*: spike-triggered average in which roughly the last 30 spikes of a total of about 50 in the synchronous switch interneuron's bursts were used (i.e., the first 20 spikes in the bursts were discarded). Delay between the spikes in the G5 switch interneuron and the average X-mediated IPSC (peak) in the G3 motor neuron is 193.5 ms.

interneurons thus form an important nexus in the circuit. Moreover, the switch interneurons introduce the side-to-side asymmetry into the system that gives rise to the asymmetric intersegmental activity pattern of the premotor interneurons, therefore of the heart motor neurons and therefore of the hearts. Rather than both being rhythmically active with beat timing, the activity of one switch interneuron is persistently suppressed (Gramoll et al. 1994) for a period corresponding to roughly 20–40 beat cycles. After this interval the neurons exchange roles and the pattern generator switches coordination states simultaneously side to side. It was shown previously that these switches are regular and periodic at the level of heart contractions, motor neurons, and interneurons (Calabrese 1977; Gramoll et al. 1994; Krahl and Zerbst-Boroffka 1983; Lu et al. 1999; Wenning et al. 2004a,b). Thus it has been hypothesized that the switch interneurons are controlled by an independent switch oscillator with a period roughly 20 to 40 times longer than the beat period (Gramoll et al. 1994; Lu et al. 1999). The bilateral link of the switch interneurons to the rear premotor interneurons guarantees side-to-side asymmetry in the output and thus the asymmetric intersegmental pattern of premotor output of the heartbeat CPG can be ascribed to the switch interneurons and the rear premotor interneurons. Thus beat rhythm and asymmetric intersegmental patterned output are separated. Intersegmental pattern and rhythm do overlap, however, in that the front premotor interneurons provide intersegmental input, albeit strictly symmetric, to the motor neurons. We also know now that the oscillator heart interneurons of G3 and G4 (also front premotor interneurons) can burst endogenously when pharmacologically isolated (Cymbalyuk et al. 2002), but the timing network module is so tightly interconnected that it does function as a unified oscillatory network (Masino and Calabrese 2002a,b,c).

Although such a separation of rhythm and pattern generation has often been the subject of analysis and theory in vertebrate systems it is rarely discussed in the well-described motor pattern generators of invertebrates. In the pyloric pattern generator of the crustacean stomatogastric ganglion, rhythm generation has been relegated to the pacemaker group of AB and PD cells and pattern to this core's synaptic interactions with motor neurons (Hooper and Marder 1987; Marder et al. 2005); in the more complex gastric mill pattern generator no core oscillator or other core network has been identified that is active in all the various modulatory permutations of its output (Hooper and DiCaprio 2004; Marder and Bucher 2001; Nusbaum and Beenhakker 2002). The stomatogastric pattern generators have always presented an ambiguous model for such a separation of function because, unlike most other pattern generators, motor neurons are key components in elaborating both rhythm and pattern. Moreover, it is clear in the gastric mill network that "descending modulatory inputs" are important elements in rhythm generation (Hooper and DiCaprio 2004; Marder and Bucher 2001; Nusbaum and Beenhakker 2002). Clear separation between local interneurons concerned with rhythm generation and local motor patterning (Paul and Mulloney 1985) and interneurons involved in intersegmental coordination (i.e., elaborating intersegmental pattern) appears to occur in the swimmeret system of crayfish; these coordinating interneurons are not apparently premotor, however (Mulloney and Hall 2003; Mulloney et al. 1998, 2006). In the leech swimming central pattern generator, rhythm generation, local pattern elaboration, and intersegmental coordination are all shared by key network interneurons (Kristan et al. 2005), although intersegmental coordination relies heavily on sensory feedback (Cang and Friesen 2000, 2002). In vertebrate systems, there has been an evolution of thinking about the origins of rhythm generation and recent studies have emphasized modular organization with unit burst generators that produce rhythmic activity, and modular interconnections and sensory feedback that produce pattern (e.g., Cangiano and Grillner 2003, 2005; Hellgren-Kotaleski 1999a,b; Stein 2005). In the lamprey swim pattern generator, a long-standing effort has yielded the most complete description of interneuronal activity

pattern in a vertebrate (for recent reviews see De Schutter et al. 2005; Grillner et al. 2005).

Major identified classes of interneurons appear to be premotor, involved in rhythm generation, and potentially in intersegmental coordination. Recent studies have emphasized, however, that local excitatory interneurons may constitute burst generating modules with crossed inhibition functioning mainly to set up a side-to-side alternating pattern and to provide intersegmental coordination (Cangiano and Grillner 2003, 2005). In other vertebrate systems, we are now seeing a concerted attempt to identify pattern generator elements and define their activity pattern [e.g., neonatal rodent locomotor pattern generator (Butt and Kiehn 2003; Butt et al. 2002; Kiehn and Butt 2003; Kiehn and Kullander 2004) and turtle hind limb pattern generators (Stein 2005)]. In turtle hind limb control, especially with respect to the scratch reflex, the concept of modular organization is well developed (Stein 2005), but because of overlap in function between interneurons and difficulties in identifying units across preparations it does not have the distinct cellular definition we present here for leech heartbeat CPG (Stein 2005). The fact that the leech heartbeat CPG is a system completely dedicated to one ongoing motor program (albeit in two alternating coordination modes) from the level of the muscles all the way to the level of the interneurons of the pattern generator has made this functional dissection a much easier process.

### *Stereotypy and phase constancy in central pattern generator output*

The activity pattern of the heartbeat CPG is quite variable across preparations (Figs. 3 and 7) but this variability does not obscure a discernable average, stereotypical pattern of intersegmental coordination that can unambiguously define synchronous and peristaltic output over a broad range of periods. These assertions are supported by the correlational analysis of Fig. 3 and by significant differences in activity phase that correspond to synchronous and peristaltic phasing of the rear premotor interneurons (Fig. 7). Moreover, there are significant differences in duty cycle across neurons and coordination mode (Tables 1, 2, and 3). The switch interneurons also clearly have two distinct levels of activity corresponding to the coordination modes, being active with accelerating bursts on the synchronous side and only sporadically active on the peristaltic side. The example of Fig. 2 was chosen because it lies within one SD of the mean for all phases and duty cycles and thus represents a pattern of activity that is both typical and can be reasonably expected to generate a "typical" pattern of motor neuron activity. Other typical and some "not so typical" activity patterns can be drawn from our data set. Such average and typical data can be important in developing models of the system aimed at explaining the elaboration and intersegmental coordination of the fictive motor program in motor neurons and its phase constancy.

The pyloric pattern generator of the lobster stomatogastric has also been the subject of an exhaustive analysis and has been found to show stereotypy and phase constancy similar to that seen here (Bucher et al. 2005). This analysis has been limited to the core pattern generator. A less extensive but more inclusive analysis of the pyloric pattern showed that considering peripheral elements adds complexity to the concept of phase constancy (Hooper 1997a,b). This analysis suggests that duty cycle is not preserved over changes in cycle period because the beginning phase and end phase of the bursts of even core neurons appear to be independently regulated. In the heartbeat CPG duty cycle shows apparent phase constancy (Fig. 3). The pyloric motor pattern, moreover, does not show alternative outputs and is generated in large part by motor neurons. Other pattern generators have alternative outputs, such as the *Aplysia* feeding system, where egestive and ingestive bites have been distinguished (Cropper et al. 2004) and turtle hind limb scratch, where different areas of the body surface are the target of the scratch (Stein 2005).

In each case the different forms require different motor neuron coordinations but appear to share the fundamentals of rhythm generation. In the *Aplysia* feeding system, these coordinations are well documented at the level of activity in identified interneurons, whereas for turtle scratch and hind limb swimming movements different couplings between pattern-generating modules are postulated. In both cases, however, although distinct switches in coordinations are observed, much emphasis has been placed on the demonstration that intermediate coordination states exist and even grade into one another and that the realization of coordination mode is determined by internal state and sensory stimulation, e.g., seemingly more by the site of irritation in the case of turtle scratch (Stein 2005) and more by internal state (sensory history) in the case of *Aplysia* feeding (Lum et al. 2005; Zhurov et al. 2005). Indeed in the hind limb of the turtle even hybrids between scratch and hind limb swimming patterns are observed. The *Aplysia* feeding system has been further analyzed in terms of circuit modules composed of identified interneurons that are linked flexibly to produce different feeding associated movements such as egestive and ingestive biting (Jing et al. 2004). In the leech heartbeat CPG, the two coordination states appear to be distinct, the transitions between them precipitous, and at least in the isolated nervous system they are not stimulus driven. Moreover, the pattern of switching is very similar in intact preparations when the activity of the hearts is monitored (Krahl and Zerbst-Boroffka 1983; Wenning et al. 2004a).

### *Translating the output of the central pattern generator to the fictive motor pattern*

At present we cannot directly determine the activity of the X heart interneurons. Our indirect methods, however, give a reasonably accurate measurement of the X activity phase (Fig. 10) and at least a lower estimate of duty cycle and intraburst spike frequency (Fig. 9; Table 3), which enables us to specify completely the pattern of inhibitory inputs to motor neurons in G3–G15 [there is some circumstantial evidence of unidentified inputs to motor neurons in segments more rearward than G15 (G16–G18) (Thompson and Stent 1976b)]. It is thus instructive to ask whether the phase progressions observed in the peristaltic and synchronous mode in the premotor interneurons (excluding and including the X interneurons) are comparable to those observed in segments 3–15 for the fictive motor pattern. For the fictive motor program (heart motor neurons) on the peristaltic side (P) for G3 to G15 segmental heart motor neurons, there is a rear-to-front phase progression of 61.8% (+61.8% phase difference), whereas for the same motor neurons on the synchronous side (S), there is a front-to-rear phase

progression of 20.0% (−20.0% phase difference) (Wenning et al. 2004b). On the synchronous side, the phase progression available in the output of the premotor interneurons of the heartbeat CPG including the X interneuron, considering the "front-to-rear" firing sequence [HN(S,X), HN(S,4), HN(S,3), HN(S,6), HN(S,7)], is −34.7% (Tables 1 and 3). Ignoring the X interneuron, this difference becomes −6.8%. In other words, considering the X interneuron at least, there is more than enough phase range in premotor output (−34.7%) to account for the motor neuron phase progression (−20.0%), suggesting that the X interneuron is important for motor neuron phasing on the synchronous side.

On the peristaltic side, the phase progression available in the output of the premotor interneurons of the heartbeat CPG including the X interneuron, considering the "rear-to-front" firing sequence [HN(P,7), HN(P,6), HN(P,4), HN(P,3), HN(P,X)], is +41.3% (Tables 1 and 3). Ignoring the X interneuron this difference becomes +22.1%. In other words, even considering the X interneuron there is not enough phase range in premotor output (+41.3%) to account for the motor neuron phase progression (+61.8%). The situation becomes much worse (+22.1 vs. +61.8%), if we ignore the X interneuron, suggesting that the X interneuron is critically important for motor neuron phasing on the peristaltic side. The large discrepancy between premotor phase range and motor neuron phase progression, especially on the peristaltic side, suggests that we will have to determine not only both the intersegmental differences in strength and dynamics of all premotor interneuron synaptic inputs onto motor neurons but also the intrinsic properties of the motor neurons (with potential intersegmental differences; see, e.g., Opdyke et al. 1995) to uncover the mechanisms that can transform the smaller phase progression of the interneurons into the larger phase progression of the motor neurons on the peristaltic side and the larger phase progression of the interneurons into the smaller phase progression of the motor neurons on the synchronous side. In general, it seems likely that analysis of the premotor input activity pattern must be followed by further analysis before we can understand how this or any other motor program is produced from CPG output, although modeling may be a useful way to identify the key parameters that must be determined.

## ACKNOWLEDGMENTS

Present address of A. L. Weaver: Department of Otolaryngology, University of Washington, Seattle, WA 98105–6515.

## GRANTS

This work was supported by National Institute of General Medical Sciences Institutional Research and Academic Career Development postdoctoral fellowships GM-000680 to L. G. Morris and A. L. Weaver and by National Institute of Neurological Disorders and Stroke Grant NS-24072 to R. L. Calabrese.

## REFERENCES

**Bucher D, Prinz AA, and Marder E.** Animal-to-animal variability in motor pattern production in adults and during growth. *J Neurosci* 25: 1611–1619, 2005.

**Butera RJ Jr, Rinzel J, and Smith JC.** Models of respiratory rhythm generation in the pre-Botzinger complex. I. Bursting pacemaker neurons. *J Neurophysiol* 82: 382–397, 1999a.

**Butera RJ Jr, Rinzel J, and Smith JC.** Models of respiratory rhythm generation in the pre-Botzinger complex. II. Populations of coupled pacemaker neurons. *J Neurophysiol* 82: 398–415, 1999b.

**Butt SJ, Harris-Warrick RM, and Kiehn O.** Firing properties of identified interneuron populations in the mammalian hindlimb central pattern generator. *J Neurosci* 22: 9961–9971, 2002.

**Butt SJ and Kiehn O.** Functional identification of interneurons responsible for left-right coordination of hindlimbs in mammals. *Neuron* 38: 953–963, 2003.

**Calabrese RL.** The neural control of alternate heartbeat coordination states in the leech, *Hirudo medicinalis*. *J Comp Physiol A Neuroethol Sens Neural Behav Physiol* 122: 111–143, 1977.

**Calabrese RL.** The roles of endogenous membrane properties and synaptic interaction in generating the heartbeat rhythm of the leech, *Hirudo medicinalis*. *J Exp Biol* 82: 163–176, 1979.

**Calabrese RL and Peterson E.** Neural control of heartbeat in the leech, *Hirudo medicinalis*. *Symp Soc Exp Biol* 37: 195–221, 1983.

**Cang J and Friesen WO.** Sensory modification of leech swimming: rhythmic activity of ventral stretch receptors can change intersegmental phase relationships. *J Neurosci* 20: 7822–7829, 2000.

**Cang J and Friesen WO.** Model for intersegmental coordination of leech swimming: central and sensory mechanisms. *J Neurophysiol* 87: 2760–2769, 2002.

**Cangiano L and Grillner S.** Fast and slow locomotor burst generation in the hemispinal cord of the lamprey. *J Neurophysiol* 89: 2931–2942, 2003.

**Cangiano L and Grillner S.** Mechanisms of rhythm generation in a spinal locomotor network deprived of crossed connections: the lamprey hemicord. *J Neurosci* 25: 923–935, 2005.

**Cropper EC, Evans CG, Hurwitz I, Jing J, Proekt A, Romero A, and Rosen SC.** Feeding neural networks in the mollusc *Aplysia*. *Neurosignals* 13: 70–86, 2004.

**Cymbalyuk GS, Gaudry Q, Masino MA, and Calabrese RL.** Bursting in leech heart interneurons: cell-autonomous and network-based mechanisms. *J Neurosci* 22: 10580–10592, 2002.

**Del Negro CA, Johnson SM, Butera RJ, and Smith JC.** Models of respiratory rhythm generation in the pre-Botzinger complex. III. Experimental tests of model predictions. *J Neurophysiol* 86: 59–74, 2001.

**De Schutter E, Ekeberg O, Kotaleski JH, Achard P, and Lansner A.** Biophysically detailed modelling of microcircuits and beyond. *Trends Neurosci* 28: 562–569, 2005.

**Gramoll S, Schmidt J, and Calabrese RL.** Switching in the activity state of an interneuron that controls coordination of the hearts in the medicinal leech (*Hirudo medicinalis*). *J Exp Biol* 186: 157–171, 1994.

**Grillner S.** Control of locomotion in bipeds, tetrapods, and fish. In: *Handbook of Physiology*. *The Nervous System*. *Motor Control*. Bethesda, MD: Am. Physiol. Soc., 1981, sect. 1, vol. II, pt. 2, p. 1179–1236.

**Grillner S.** The motor infrastructure: from ion channels to neuronal networks. *Nat Rev Neurosci* 4: 573–586, 2003.

**Grillner S, Markram H, De Schutter E, Silberberg G, and LeBeau FE.** Microcircuits in action—from CPGs to neocortex. *Trends Neurosci* 28: 525–533, 2005.

**Hellgren-Kotaleski J, Grillner S, and Lansner A.** Neural mechanisms potentially contributing to the intersegmental phase lag in lamprey. I. Segmental oscillations dependent on reciprocal inhibition. *Biol Cybern* 81: 317–330, 1999a.

**Hellgren-Kotaleski J, Lansner A, and Grillner S.** Neural mechanisms potentially contributing to the intersegmental phase lag in lamprey. II. Hemisegmental oscillations produced by mutually coupled excitatory neurons. *Biol Cybern* 81: 299–315, 1999b.

**Hildebrandt K-P.** Circulation in the leech, *Hirudo medicinalis*. *J Exp Biol* 134: 235–246, 1988.

**Hill AA, Masino MA, and Calabrese RL.** Model of intersegmental coordination in the leech heartbeat neuronal network. *J Neurophysiol* 87: 1586–1602, 2002.

**Hooper SL.** Phase maintenance in the pyloric pattern of the lobster (*Panulirus interruptus*) stomatogastric ganglion. *J Comput Neurosci* 4: 191–205, 1997a.

**Hooper SL.** The pyloric pattern of the lobster (*Panulirus interruptus*) stomatogastric ganglion comprises two phase-maintaining subsets. *J Comput Neurosci* 4: 207–219, 1997b.

**Hooper SL and DiCaprio RA.** Crustacean motor pattern generator networks. *Neurosignals* 13: 50–69, 2004.

**Hooper SL and Marder E.** Modulation of the lobster pyloric rhythm by the peptide proctolin. *J Neurosci* 7: 2097–2112, 1987.

**Hurwitz I and Susswein AJ.** B64, a newly identified central pattern generator element producing a phase switch from protraction to retraction in buccal

motor programs of *Aplysia californica*. *J Neurophysiol* 75: 1327–1344, 1996.

**Jing J, Cropper EC, Hurwitz I, and Weiss KR.** The construction of movement with behavior-specific and behavior-independent modules. *J Neurosci* 24: 6315–6325, 2004.

**Katz PS, Sakurai A, Clemens S, and Davis D.** Cycle period of a network oscillator is independent of membrane potential and spiking activity in individual central pattern generator neurons. *J Neurophysiol* 92: 1904–1917, 2004.

**Kiehn O and Butt SJ.** Physiological, anatomical and genetic identification of CPG neurons in the developing mammalian spinal cord. *Prog Neurobiol* 70: 347–361, 2003.

**Kiehn O and Kullander K.** Central pattern generators deciphered by molecular genetics. *Neuron* 41: 317–321, 2004.

**Krahl B and Zerbst-Boroffka I.** Blood pressure in the leech *Hirudo medicinalis*. *J Exp Biol* 107: 163–168, 1983.

**Kristan WB Jr, Calabrese RL, and Friesen WO.** Neuronal control of leech behavior. *Prog Neurobiol* 76: 279–327, 2005.

**Lu J, Gramoll S, Schmidt J, and Calabrese RL.** Motor pattern switching in the heartbeat pattern generator of the medicinal leech: membrane properties and lack of synaptic interaction in switch interneurons. *J Comp Physiol A Sens Neural Behav Physiol* 184: 311–324, 1999.

**Lum CS, Zhurov Y, Cropper EC, Weiss KR, and Brezina V.** Variability of swallowing performance in intact, freely feeding *Aplysia*. *J Neurophysiol* 94: 2427–2446, 2005.

**Maranto AR and Calabrese RL.** Neural control of the hearts in the leech, *Hirudo medicinalis*. I. Anatomy, electrical coupling, and innervation of the hearts. *J Comp Physiol A Sens Neural Behav Physiol* 154: 367–380, 1984a.

**Maranto AR and Calabrese RL.** Neural control of the hearts in the leech, *Hirudo medicinalis*. II. Myogenic activity and its control by heart motor neurons. *J Comp Physiol A Sens Neural Behav Physiol* 154: 381–391, 1984b.

**Marder E and Bucher D.** Central pattern generators and the control of rhythmic movements. *Curr Biol* 11: R986–R996, 2001.

**Marder E, Bucher D, Schulz DJ, and Taylor AL.** Invertebrate central pattern generation moves along. *Curr Biol* 15: R685–R699, 2005.

**Marder E and Calabrese RL.** Principles of rhythmic motor pattern generation. *Physiol Rev* 76: 687–717, 1996.

**Masino MA and Calabrese RL.** Phase relationships between segmentally organized oscillators in the leech heartbeat pattern generating network. *J Neurophysiol* 87: 1572–1585, 2002a.

**Masino MA and Calabrese RL.** Period differences between segmental oscillators produce intersegmental phase differences in the leech heartbeat timing network. *J Neurophysiol* 87: 1603–1615, 2002b.

**Masino MA and Calabrese RL.** A functional asymmetry in the leech heartbeat timing network is revealed by driving the network across various cycle periods. *J Neurosci* 22: 4418–4427, 2002c.

**Mulloney B and Hall WM.** Local commissural interneurons integrate information from intersegmental coordinating interneurons. *J Comp Neurol* 466: 366–376, 2003.

**Mulloney B, Harness PI, and Hall WM.** Bursts of information: coordinating interneurons encode multiple parameters of a periodic motor pattern. *J Neurophysiol* 95: 850–861, 2006.

**Mulloney B, Skinner FK, Namba H, and Hall WM.** Intersegmental coordination of swimmeret movements: mathematical models and neural circuits. *Ann NY Acad Sci* 860: 266–280, 1998.

**Nusbaum MP and Beenhakker MP.** A small-systems approach to motor pattern generation. *Nature* 417: 343–350, 2002.

**Opdyke CA and Calabrese RL.** Outward currents in heart motor neurons of the medicinal leech. *J Neurophysiol* 74: 2524–2537, 1995.

**Paul DH and Mulloney B.** Nonspiking local interneuron in the motor pattern generator for the crayfish swimmeret. *J Neurophysiol* 54: 28–39, 1985.

**Peterson EL and Calabrese RL.** Dynamic analysis of a rhythmic neural circuit in the leech *Hirudo medicinalis*. *J Neurophysiol* 47: 256–271, 1982.

**Rybak IA, Shevtsova NA, Paton JF, Dick TE, St-John WM, Morschel M, and Dutschmann M.** Modeling the ponto-medullary respiratory network. *Respir Physiol Neurobiol* 143: 307–319, 2004b.

**Rybak IA, Shevtsova NA, Paton JF, Pierrefiche O, St-John WM, and Haji A.** Modelling respiratory rhythmogenesis: focus on phase switching mechanisms. *Adv Exp Med Biol* 551: 189–194, 2004a.

**Stein PS.** Neuronal control of turtle hindlimb motor rhythms. *J Comp Physiol A Neuroethol Sens Neural Behav Physiol* 191: 213–229, 2005.

**Straub VA, Staras K, Kemenes G, and Benjamin PR.** Endogenous and network properties of Lymnaea feeding central pattern generator interneurons. *J Neurophysiol* 88: 1569–1583, 2002.

**Thompson WJ and Stent GS.** Neuronal control of heartbeat in the medicinal leech. I. Generation of the vascular constriction rhythm by heart motor neurons. *J Comp Physiol* 111: 261–279, 1976a.

**Thompson WJ and Stent GS.** Neuronal control of heartbeat in the medicinal leech. II. Intersegmental coordination of heart motor neuron activity by heart interneurons. *J Comp Physiol* 111: 281–307, 1976b.

**Thompson WJ and Stent GS.** Neuronal control of heartbeat in the medicinal leech. III. Synaptic relations of the heart interneurons. *J Comp Physiol* 111: 309–333, 1976c.

**Tunstall MJ, Roberts A, and Soffe SR.** Modelling inter-segmental coordination of neuronal oscillators: synaptic mechanisms for uni-directional coupling during swimming in Xenopus tadpoles. *J Comput Neurosci* 13: 143–158, 2002.

**Wenning A and Calabrese RL.** Uncovering the phase and strength of unidentified rhythmic inhibitory inputs to motor neurons by the leech heartbeat CPG. *Soc Neurosci Abstr* 31: 54.2, 2005.

**Wenning A, Cymbalyuk GS, and Calabrese RL.** Heartbeat control in leeches. I. Constriction pattern and neural modulation of blood pressure in intact animals. *J Neurophysiol* 91: 382–396, 2004a.

**Wenning A, Hill AA, and Calabrese RL.** Heartbeat control in leeches. II. Fictive motor pattern. *J Neurophysiol* 91: 397–409, 2004b.

**Zhurov Y, Proekt A, Weiss KR, and Brezina V.** Changes of internal state are expressed in coherent shifts of neuromuscular activity in Aplysia feeding behavior. *J Neurosci* 25: 1268–1280, 2005.